21

ИНСТИТУТ ЯДЕРНОЙ ФИЗИКИ
СО АН СССР

I.F.Ginzburg, G.L.Kotkin, V.G.Serbo,
V.I.Telnov

COLLIDING γe - AND $\gamma\gamma$ -BEAMS BASED ON THE SINGLE-PASS ACCELERATORS (OF VLEPP TYPE)

Preprint 81 - 102

Новосибирск

Institute of Nuclear Physics
630090, Novosibirsk 90, USSR

I.F.Ginzburg*, G.L.Kotkin**, V.G.Serbo**
V.I.Telnov

COLLIDING γe - AND $\gamma\gamma$ -BEAMS BASED
ON THE SINGLE-PASS ACCELERATORS
(OF VLEPP TYPE)

* Institute of Mathematics, Novosibirsk
** Novosibirsk State University

Preprint 81-102

Novosibirsk
1981

Abstract

We discuss in detail our proposed [1,2] method of obtaining colliding γe - and $\gamma\gamma$ - beams with high energies and luminosities using the designed linear accelerators VLEPP and SLC with colliding e^+e^- - beams at the energies $2E \gtrsim 100$ GeV. The intense γ - beams are obtained by backward Compton scattering of laser light which is focused on the electron beams of these accelerators. This paper contains the scheme for conversion of an electron beam into a γ - beam, the calculation of the conversion coefficient and of the total and spectral γe - and $\gamma\gamma$ - luminosities. To get the luminosity $L_{\gamma e}$, $L_{\gamma\gamma} \sim L_{ee}$, one needs a laser flash with energy ~ 15 J, and a pulse duration ~ 30 ps at a repetition rate of 10 or 180 Hz. Such parameters seem to be achievable on the basis of the current technology.

The luminosity distribution over the γe - or $\gamma\gamma$ - invariant mass is broad. Offered is the method of monochromatization. It demands an increase of the laser flash energy (with a possible increase of pulse duration) and leads to a decrease of luminosity.

We also describe a method for calibrating the total and spectral luminosities.

The background problems are shown to be easier than in e^+e^- - collisions. Some examples of interesting physical problems for γe - and $\gamma\gamma$ - collisions are enumerated.

I. INTRODUCTION

1. In the brief communications [1,2]* we show that, using the designed linear e^+e^- - colliders V L E P P [4] and S L C [5], one can obtain colliding γe - and $\gamma\gamma$ - beams with approximately the same energies ($\gtrsim 100$ GeV) and luminosities ($\sim 10^{30} \div 10^{32}$ cm^{-2}c^{-1}) as e^+e^- -collisions.

This paper contains a detailed description of the conversion of an electron beam into a γ -beam, the calculation of the conversion coefficient, the main characteristics of the γe - and $\gamma\gamma$ - collisions and the problems of background and luminosity calibration.

2. The $\gamma\gamma$- and γe - collisions are presently studied on the e^+e^- - accelerators in the reactions $e^+e^- \to e^+e^- \gamma^*\gamma^* \to e^+e^- X$, where the γ^* is virtual photon (see, e.g. [6]). The continuation of such experiments is planned for the accelerators of the next generation [7,8]. However, the effective luminosities of those $\gamma^*\gamma^*$- and $\gamma^* e$ - collisions is considerably lower than the luminosity of the e^+e^- - collisions. The proposed direct $\gamma\gamma$ - and γe - collisions will allow one to continue the investigation of the same problems as in virtual photon collision and at the same time, will permit new studies of objects which are practically inaccessible by other methods**. One may make, for example, a detailed investigation of $W^\pm$ - bosons and their gauge vertices in the reactions $\gamma e \to W\nu$, $\gamma\gamma \to W^+W^-$, $\gamma e \to WZ\nu$ of perturbative pomeron structure in QCD, of gluon jets ($\gamma\gamma \to gg$), of photon structure functions in the nontrivial parameter range, of the nature of the total cross section growth at high energy, and of possible new particles, etc.

---

* The main results of these papers are contained in report [3].

** This is due to the large luminosity as well as to a better background conditions with the proposed scheme. The comparison of this scheme with the equivalent photon scheme is given in Appendix A.

Therefore, the physical problems which can be investigated with these devices are no less interesting than those in the e^+e^- - collisions. They, in fact, represent an important addition to the problems which are studied in pp, $p\bar{p}$, ep and e^+e^- - collisions.

3. The paper is organized as follows. In sect. 2 the scheme for obtaining the γ - beams is described and an estimation of the conversion coefficient of electrons into photons is given. In sect. 3 the energy and angular distribution of the high-energy photons are described and the possibility of their polarization is discussed. The conversion coefficient for different bunch parameters is calculated in sect. 5. In sect 6 the total luminosities $L_{\gamma e}$, $L_{\gamma\gamma}$ and the luminosity distribution over the total c.m.s. energy of colliding particles is calculated. Since the W -distribution is quite broad, a monochromatization of these collisions is useful for the detailed investigation of the W - dependence. Such a possibility is discussed in sect. 7. When the laser flash energy is large, some other processes in the conversion region become important (besides the basic Compton effect). Their role is discussed in sect 8. The results obtained are illustrated by a number of examples for SLC and VLEPP in sect. 9. In sect. 10 the possibilities of using this scheme with the different type of the lasers is discussed as well as the possibilities connected with a change of the electron bunch parameters.

It is known that background conditions for experiments with the colliding e^+e^- - beams of V L E P P and S L C are rather difficult [4,5,8]. For the proposed γe - and $\gamma\gamma$ - - collisions this problem is easier. In Appendix B the main background processes are discussed and it is shown that they are not dangerous.

The proposed scheme demands the calibration of the total as well as spectral luminosity. A method for such a calibration is suggested in Appendix C.

Having completed the present paper we received the preprint by C.Akerlof "Using the S L C as a photon accelerator" (University of Michigan, UM HE 81-59) which appeared after our paper [1] and report [3]. He has proposed the scheme which is

similar to ours. However, his estimations of the laser energy are too optimistic (his values of the laser flash energy are 10-100 times lower than the correct ones).

2. THE PROPOSED SCHEME. PRELIMINARY ESTIMATIONS

1. It is clear now that obtaining of colliding e^+e^- - - beams with the energy $E \gtrsim 100$ GeV is most perspective at linear accelerators [9]. Such machines are being designed now in Novosibirsk (VLEPP, $E = 100 \div 300$ GeV [4]) and in Stanford (SLAC Linear Collider or S L C, $E = 50 \div 70$ GeV [5]). To obtain the γe - and $\gamma\gamma$ - beams, the next features of these devices are important:

a) the bunches will only be used once*;

b) the repetition rate of the accelerator cycles is not too large (ν = 10 Hz [4] or 180 Hz [5]);

c) the high luminosity of these devices $L_{ee} = \nu N_{e^+} N_{e^-} / S_{eff} \sim 10^{32}$ cm^{-2} c^{-1} will be provided by means of the very small bunch size (the effective beam cross section at the interaction point $S_{eff} = (1 \div 2)\cdot 10^{-7}$ cm^2, the bunch length ℓ_e = $= 2 \div 3.6$ mm) and the large number of particles $N_{e^\pm}$ in bunches.

2. On the VLEPP and SLC the electron bunches are prepared for every collision anew. Hence, if one succeeds to convert all electrons into photons and one conserves the beam size, then the luminosity of the γe - and $\gamma\gamma$ - collisions will be the same as for e^+e^- - collisions (moreover, this luminosity can even be larger, in principle, than in the e^+e^- - collisions, because the e^+e^- - luminosity is restricted by the effects of beam-beam interaction which are absent in the γe - or $\gamma\gamma$ - collisions).

---

* It is the main feature which distinguishes these accelerators from the usual e^+e^- - storage rings. In the latter high luminosity is provided by a number of collisions ($\sim 10^9 \div 10^{11}$) of the e^+ and e^- - bunches. If one converts the electron bunch into the γ -bunch on such accelerators, we will have one collision of the γe - or $\gamma\gamma$ -bunches only. As a result, the luminosity of the γe - or $\gamma\gamma$ - collisions will become less by a factor 10^8-10^{10}, which is a ratio of a storage time to a revolution time.

The photons of high energy $\omega \sim E$ are suggested to be obtained by backward Compton scattering of laser light which is focused on an electron beam. Such a method is well known [10] and has been realized, e.g., in refs. [11,12]. However, the conversion coefficient of electrons to photons k was very small in all these experiments. For example, in ref. [12] $k \sim 10^{-7}$. In our papers [1,2] it was found out that a small size of electron bunches of the VLEPP and SLC will allow one to get high enough photon density (to provide $k \sim 1$) at a moderate laser flash energy $A \sim 15$ J.

3. <u>The proposed scheme</u> is shown in fig. 1: the laser light is focused on an electron beam in the conversion region C at some distance $b \sim 10$ cm from the interaction point 0; after scattering on the electrons the high-energy photons follow along initial electron trajectories, i.e. they are focused in the interaction point 0. Electrons are bent by a magnetic field $B \sim 1$T. The obtained γ -beam is collided downstream with the oppositely directed electron or the similar γ -beam.

Let us now estimate the conversion coefficient k. If a laser bunch is focused in such a way that the area of a focal spot S coincides with the area of electron bunch cross section in the conversion region, then it is sufficient to have S/σ_c photons to overlap this area and to provide $k \sim 1$ (σ_c is the Compton total cross section). The laser pulse energy needed for this aim is

$$A_0 \sim \frac{S}{\sigma_c}\,\omega_0 \qquad (1)$$

where ω_0 is the energy of the laser photon (it is assumed that the electron and γ -beams are short enough. If the laser pulse energy A is considerably less than A_0, the conversion coefficient

$$k = \frac{A}{A_0} \qquad (2)$$

For estimations we use below

$\omega_0 = 1.17$ eV ($\lambda = 1.06\,\mu$m, neodymium glass laser). (3)

At E = 50 ÷ 300 GeV the Compton cross section is

$$\sigma_c = (2 \div 4)\cdot 10^{-25}\ cm^2.$$

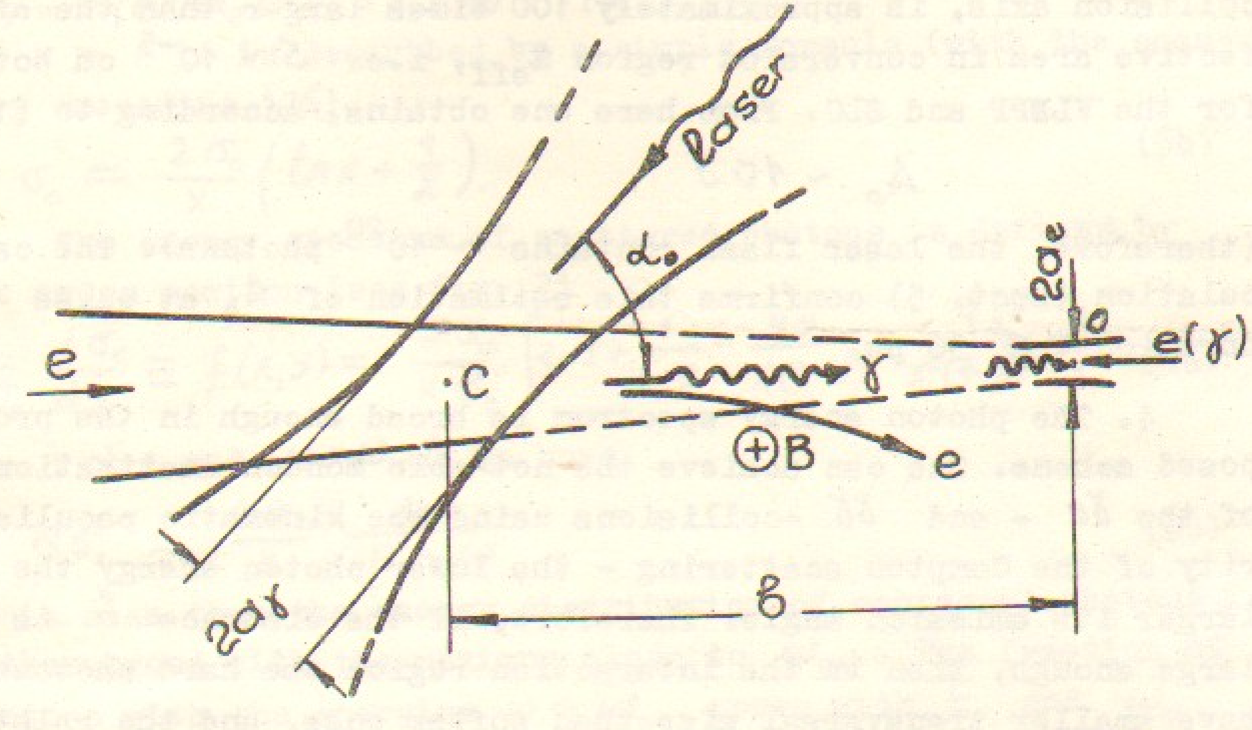

<u>Fig.1</u>. Scheme of obtaining of the colliding γe - and $\gamma\gamma$ -beams.

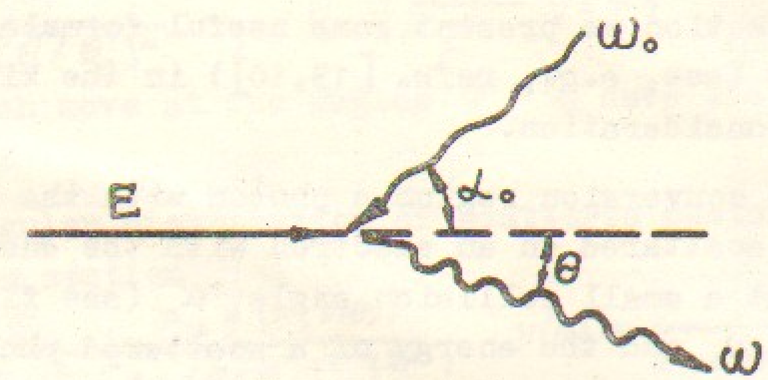

<u>Fig.2.</u> Kinematics of the Compton scattering.

At b = 10 cm the electron bunch area S, transverse to the collision axis, is approximately 100 times larger than the effective area in conversion region S_{eff}, i.e. $S \sim 10^{-5}$ cm both for the VLEPP and SLC. From here one obtains, according to (1),

$$A_o \sim 10\,J$$

(therefore, the laser flash contains $\sim 10^{20}$ photons). The calculation (sect. 5) confirms this estimation of A_o at pulse duration $\tau \lesssim$ 30 ps.

4. The photon energy spectrum is broad enough in the proposed scheme. One can achieve the not-able monochromatization of the γe - and $\gamma\gamma$ -collisions using the kinematic peculiarity of the Compton scattering - the lower photon energy the larger its emission angle. Therefore, if the distance b is large enough, then in the interaction region the hard photons have smaller transversal size than softer ones, and the relative contribution of hard photons into luminosity increases.

3. ENERGY AND ANGULAR DISTRIBUTION AND POLARIZATION OF SCATTERED PHOTONS

In this section we present some useful formulae for the Compton effect (see, e.g., refs. [13,10]) in the kinematical region under consideration.

1. In the conversion region a photon with the energy $\omega_o \sim$ 1 eV is scattered on an electron with the energy E $\sim$ 100 GeV at a small collision angle α_o (see fig. 2). Instead of E, ω_o and the energy of a scattered photon ω it is convenient to use the dimensionless quantities

$$x = \frac{4E\omega_o}{m_e^2 c^4}\cos^2\frac{\alpha_o}{2}, \quad y = \frac{\omega}{E} \le y_m = \frac{\omega_m}{E} = \frac{x}{x+1}, \qquad (4)$$

where ω_m is the maximum energy of the scattered photon*.

The total Compton cross section is

* The quantity $m_e c^2\sqrt{x+1}$ is the total c.m.s. energy of a laser photon + an incident electron system. In the range under consideration this energy is not large, $\sim (1.3\div 3)m_e c^2$.

$$\sigma_c = \frac{2\sigma_o}{x}\left[\left(1-\frac{4}{x}-\frac{8}{x^2}\right)\ln(x+1)+\frac{1}{2}+\frac{8}{x}-\frac{1}{2(x+1)^2}\right], \qquad (5a)$$

$$\sigma_o = \pi(e^2/m_e c^2)^2 = 2.5\cdot 10^{-25}\,cm^2.$$

For $x >$ 2 it is described by a simple formula (with the accuracy exceeding 13%)

$$\sigma_c = \frac{2\sigma_o}{x}\left(\ln x + \frac{1}{2}\right). \qquad (5b)$$

The energy spectrum of scattered photons is defined by the cross section (see fig. 3)

$$\frac{1}{\sigma_c}\frac{d\sigma_c}{dy} \equiv f(x,y) = \frac{2\sigma_o}{x\sigma_c}\left[1-y+\frac{1}{1-y}-\frac{4y}{x(1-y)}+\frac{4y^2}{x^2(1-y)^2}\right] \qquad (6a)$$

For $x \gg 1$ and $\omega > \omega_m/2$ we have

$$d\sigma_c \approx \frac{2\sigma_o}{x}\,\frac{d\omega}{E-\omega} \qquad (6b)$$

It is seen that the energy distribution of scattered photons is rather broad with the maximum close to ω_m. The fraction of photons with the energies $\omega \sim \omega_m$ grows with E and ω_o growth.

The energy of a scattered photon depends on its emission angle θ relative to the motion of an incident electron (see fig. 2) as follows

$$\omega = \frac{\omega_m}{1+(\theta/\theta_o)^2}, \quad \theta_o = \frac{m_e c^2}{E}\sqrt{x+1} \qquad (7)$$

Photons which move at the angles $\theta < \theta_o$ have the energies $\omega > \omega_m/2$.

The angular distribution of scattered photons is defined by the cross section

$$\frac{d\sigma_c}{d\Omega_\gamma} = \frac{\sigma_c}{\pi\theta_o^2}\,\frac{y_m f(x,y(\theta))}{[1+(\theta/\theta_o)^2]^2}, \quad y(\theta) = \frac{y_m}{1+(\theta/\theta_o)^2}. \qquad (8)$$

It has a very sharp peak in the direction of the incident electron momentum. In the vicinity of $\theta = 0$

$$\frac{d\sigma_c(\theta)}{d\Omega_\gamma} = \frac{d\sigma_c(0)}{d\Omega_\gamma}\left(1-D\frac{\theta^2}{\theta_o^2}\right), \quad D = x+6-\frac{2x+4}{(x+1)^2+1} \approx x+6. \qquad (8a)$$

Hence, the angular size of the region of high photon density is $\sim \theta_o/\sqrt{D} \approx \theta_o/\sqrt{x+6}$.

The above formulae are illustrated in table 1. For the cases under consideration half or more of scattered photons

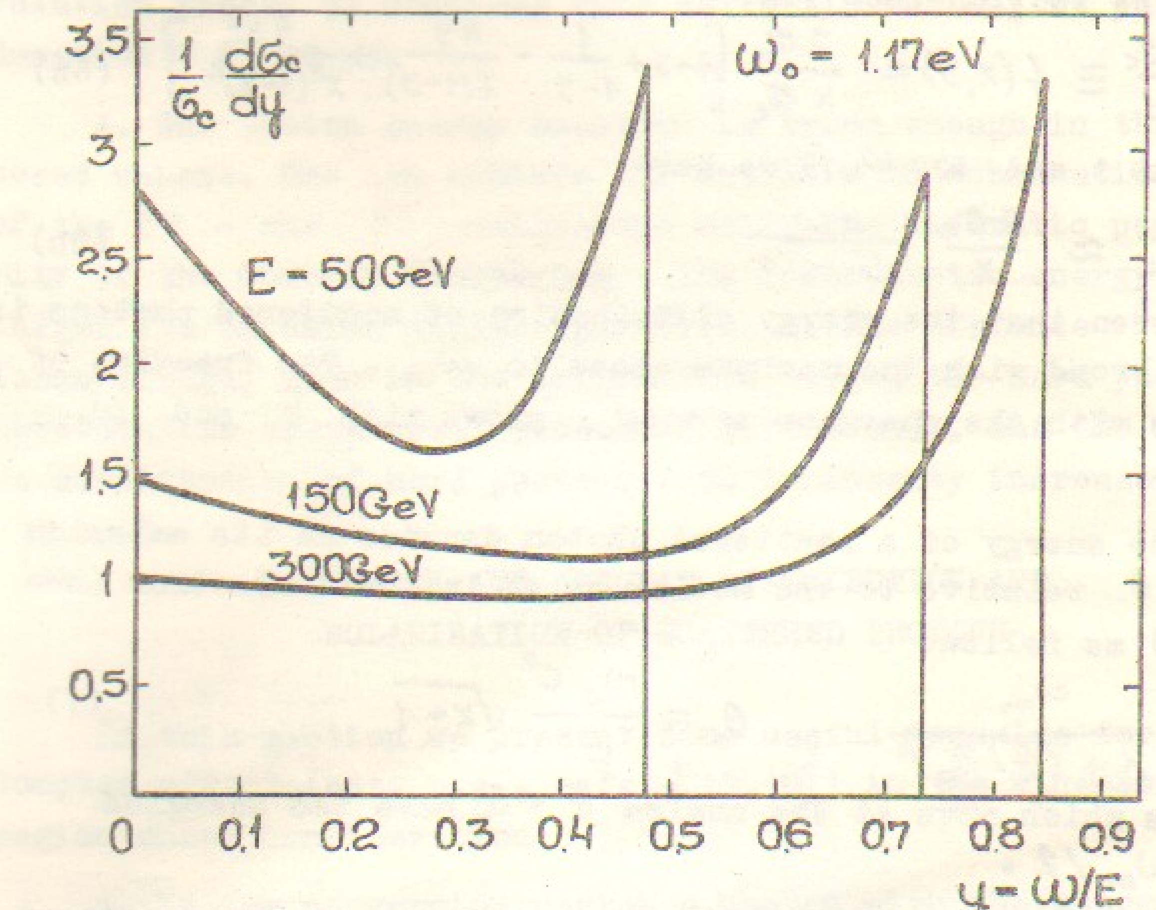

Fig.3. Energy spectrum of scattered photons.

Table 1

E, GeV	laser	$x = \frac{4E\omega_0}{m_e^2 c^4}$	ω_m, GeV	$y_m = \frac{\omega_m}{E}$	$\frac{\sigma_c}{\sigma_0}$	θ_0, 10^{-5} rad
50	Nd [a)]	0,896	24	0,47	1,56	1,4
	3 Nd [b)]	2,69	36	0,73	1,01	2,0
100	Nd	1,79	64	0,64	1,20	0,85
150	Nd	2,69	109	0,73	1,01	0,65
	3Nd	8,06	134	0,89	0,577	1,0
300	Nd	5,37	253	0,84	0,721	0,43

a) Nd - neodymium glass laser, $\omega_0 = 1.17$ eV

b) 3 Nd - neodymium glass laser with frequency tripling, $\omega_0 = 3.5$ eV.

fly into angular range $\theta < \theta_0 \lesssim 10^{-5}$ rad and their energies are $\omega > \omega_m/2 = (0.24 \div 0.45)\,E$.

2. Polarization of scattered photon. If laser light or an electron beam are polarized, then the scattered photons have considerable polarization degree ξ' as well. Table 2

Table 2

What is polarized and how		Polarization of the scattered photons
laser light	linear ξ_3	linear $\xi_3' = \xi_3 \frac{4\sigma_0}{\sigma_c x(1-y)^2 f(x,y)} \begin{cases} \frac{y^2}{x}, & y > \frac{x}{x+2}, \\ \left(1-\frac{y}{y_m}\right)^2, & y < \frac{x}{x+2} \end{cases}$
	circular ξ_2	circular $\xi_2' = \xi_2 \frac{2\sigma_0 (x+2)[1+(1-y)^2]}{\sigma_c x^2 (1-y)^2 f(x,y)} \left(\frac{x}{x+2} - y\right)$
electrons	transverse	no
	longitudinal ζ	circular $\xi_2' = \zeta \frac{2\sigma_0 y\{1-y+[1-y(x+2)/x]^2\}}{\sigma_c x(1-y)^2 f(x,y)}$

presents the ξ' values obtained after azimuthal averaging.

If the laser has the linear polarization ξ_3, the scattered photons have the linear polarization ξ_3' which has the minimum at $y = x/(x+2)$; ξ_3' decreases with x growth.

If the laser light has the circular polarization ξ_2, the scattered photons have the circular polarization ξ_2' which changes very quickly in a small y range:
$\xi_2' = -\xi_2$ at $y = y_m = x(x+1)$, $\xi_2' = 0$ at $y = x/(x+2)$, $\xi_2' \to \xi_2$ at $y \to 0$.

If the electron has the longitudinal polarization ζ, the scattered photons have the high circular polarization ξ_2' at all values of x under consideration; at $\omega > \omega_m/2$ we have $0.4\zeta < \xi_2' < \zeta$ (at $x > 2$).

4. BEAM CHARACTERISTICS

4.1. Electron beam

In the conversion scheme considered it is preferable to have electron beams with a round cross section. A density of an electron bunch n_e usually has the Gaussian character, i.e. it depends on the distance r from the axis z as $\exp(-r^2/r_e^2)$. The r.m.s. radius r_e of the electron beam at the distance b from the collision point is

$$r_e = a_e\sqrt{1 + b^2/\beta_e^2} \tag{9}$$

Here a_e is the r.m.s. radius at the interaction point O, β_e (beta function at the interaction point) is defined by the accelerator focusing system.

In all the cases considered below lengths of an electron and laser photon bunches l_e and $l_\gamma = c\tau$ are small in comparison with the distance b, so that $r_e \approx$ const in the conversion region. Therefore,

$$n_e = \frac{N_e}{\pi r_e^2} e^{-r^2/r_e^2} F_e(z - ct) \tag{10}$$

where N_e is a number of electrons in a bunch. Linear density* $F_e(z)$ is normalized by the condition

$$\int F_e(z)\,dz = 1. \tag{11}$$

It is seen from here that

$$F_e(0) \sim 1/l_e. \tag{11a}$$

* In the VLEPP project [4] $F_e(z) = \frac{1}{l}\cos^2\frac{\pi z}{2l}$ at $|z| \le l = 0.5$ cm.

We will orient ourselves to (close to each other) parameters of $e^\pm$ beams which are given in the VLEPP [4] and S L C [5] projects, see table 3.

Table 3

		VLEPP [4]	SLC [5]
Total energy 2E, GeV		200÷600	100÷140
Luminosity $L_{ee} = \nu N_{e^+} N_{e^-}/S_{eff}$, cm^{-2}s^{-1}		10^{32}	$2\cdot10^{30}$ ※)
Repetition rate ν, Hz		10	180
Number of particles/bunch,		10^{12}	$5\cdot10^{10}$
Transverse size in the collision region	S_{eff}, 10^{-7}cm^2	1	2
	$a_e = \sqrt{2}\sigma_x = \sqrt{2}\sigma_y$, μm	1,25	1,8
Bunch length, $l_e = 2\sigma_z$, cm		0,36	0,2
Beta function in the collision region β_e, cm		1	0,5

※) Without collision effects which, according to ref. [5], lead to threefold increase of the e^+e^- - luminosity.

4.2. Laser beam

To provide good focusing the Gaussian light beams are usually used in powerful lasers for which (cf.(10),(11))

$$n_\gamma = \frac{A}{\pi r_\gamma^2 \omega_0} e^{-r^2/r_\gamma^2} F_\gamma(z + ct) \tag{12}$$

(here the number of photons A/ω_0 is expressed via the laser flash energy A).

The r.m.s. radius r_γ depends on the distance z to focus and the focal spot radius a_γ in the following way (see, e.g. [14])

$$r_\gamma = a_\gamma \sqrt{1+z^2/\beta_\gamma^2} \,. \qquad (13)$$

The quantity $2a_\gamma/\beta_\gamma$ is an angular divergency of the laser beam, it is close to a relative aperture of the lense used for focusing. The laser beam cross section area at $z=\pm\beta_\gamma$ is twice as large relative to that in the focal plane (at $z=0$). In other words, $2\beta_\gamma$ is the length of the region where conversion can effectively occur. For a Gaussian shape of the beam one can realize a diffraction limit of a focusing at which [14]

$$\beta_\gamma = \frac{2\pi a_\gamma^2}{\lambda}. \qquad (14)$$

Parameters of some contemporary lasers are presented in tables 4,6,9. Point out, for example, that at $a_\gamma = 20\,\mu m$ the length $2\beta_\gamma = 0.5$ cm. At a laser flash duration $\tau = 10$ ps the length of a laser bunch $\ell_\gamma = c\tau = 0.3$ cm is comparable to that of the electron bunch.

5. CONVERSION COEFFICIENT OF ELECTRONS TO HIGH-ENERGY PHOTONS

5.1. General formulae

In this section we calculate the conversion coefficient k (i.e. the average number of high-energy photons per one electron) for the case when the energy of laser flash is not too large ($k \ll 1$). In this case a total number of electron collisions with laser photons N_{int} is defined by the well-known formulae, and

$$k = \frac{N_{int}}{N_e} = \frac{2c\sigma_c}{N_e}\int n_e n_\gamma \, dV\, dt \qquad (15)$$

Here $2c \approx |\vec{v}_e - \vec{v}_\gamma|$ is the velocity at which electrons and photons approach each other and σ_c is the total Compton cross section (5).

Since the density of laser photons n_γ is proportional to the laser flash energy A, expression (15) can be written in the

form (2) $k = A/A_0$. Therefore, the problem of k calculation is reduced to the problem of A_0 calculation.

Eq. (15) gives good approximation at $A < A_0/2$. At $A \gtrsim A_0$ the repeated collisions and other processes in the conversion region become important - see sect. 8.

Let us substitute expressions (10),(12) into eq. (15) assuming (for the simplicity) the head-on collision ($\alpha_0 = 0$) and assuming that the centers of both beams pass the focus C simultaneously (at $t=0$). After integration over radius one gets

$$k = \frac{A}{A_0}\,, \qquad A_0 = \frac{\pi}{J}\cdot\frac{r_e^2 + a_\gamma^2}{\sigma_c}\,\omega_0\,,$$

$$J = 2\int \frac{F_e(z-ct)F_\gamma(z+ct)\,dz\,c\,dt}{1+z^2/\beta_\gamma^2(1+r_e^2/a_\gamma^2)} \qquad (16)$$

Scales of $F_e(z)$ and $F_\gamma(z)$ altering are ℓ_e and ℓ_γ, therefore, J - value strongly depends on the relationship between ℓ_e, ℓ_γ and $\beta_\gamma\sqrt{1+r_e^2/a_\gamma^2}$.

5.2. Short bunches

At

$$2\beta_\gamma\sqrt{1+r_e^2/a_\gamma^2} \gg \ell_e + \ell_\gamma \qquad (17a)$$

laser bunch sizes do not vary during the conversion time, i.e. we have a collision of two cylindrical beams. The result does not depend on functions' F_e or F_γ shapes*:

$$A_0 = \frac{\pi(r_e^2 + a_\gamma^2)}{\sigma_c}\,\omega_0\,. \qquad (17b)$$

One can see that, to decrease A_0 it is useful to decrease a_γ. However, one should keep valid condition (17a). Besides, eq. (17b) is only valid for $k < a_\gamma^2/r_e^2$ (at $a_\gamma < r_e$) since only electrons travelling at the distance less than a_γ from the beam axis effectively take part in the conversion.

* In other words, under condition (17a) one can neglect the term $z^2/\beta_\gamma^2(1+r_e^2/a_\gamma^2)$ in the denominator of the integrand (16); after that integration over $z-ct$ and $z+ct$ with the account of (11) gives $J=1$.

5.3. Long electron bunch

In this case

$$\ell_e \gg \ell_\gamma ,\ 2\beta_\gamma\sqrt{1+r_e^2/a_\gamma^2} \qquad (18a)$$

and conversion occurs on the length $\sim 2\beta_\gamma$ in the vicinity of the focus during the time $\sim (\ell_\gamma+4\beta_\gamma)/c$ necessary for the laser bunch to pass this region. Hence, only $\sim N_e(\ell_\gamma+4\beta_\gamma)/\ell_e$ of electrons can take part in the conversion, i.e. the approximation (15) is only valid at $k<(\ell_\gamma+4\beta_\gamma)/\ell_e$.

From (17) one gets*

$$J = 2\pi\beta_\gamma\sqrt{1+r_e^2/a_\gamma^2}\, F_e(0). \qquad (18b)$$

From here, taking into account (14), one obtains

$$A_0 = \frac{\hbar c}{2\sigma_c F_e(0)}\sqrt{1+r_e^2/a_\gamma^2}\ . \qquad (18c)$$

Let us note that at $a_\gamma > r_e$ a value of A_0 varies only slightly with the growth of a_γ inside condition (18a), i.e. up to $a_\gamma\sim\sqrt{\lambda\ell_e/4\pi}$. This fact can be explained as follows. The probability of the electron collision with the laser photons is $k\sim\sigma_c n_\gamma \ell$, and since $n_\gamma \propto a_\gamma^{-2}$ and the conversion length is $\ell\sim\beta_\gamma\propto a_\gamma^2$ (14), then $k\approx$ const.

At $a_\gamma > r_e$ using (11a) and (18c) one obtains the convenient estimation

$$A_0 \sim \frac{\hbar c\,\ell_e}{2\sigma_c} = 6.3\,\frac{\sigma_0}{\sigma_c}\,\ell(cm)\ J. \qquad (18d)$$

5.4. Long photon bunch

In this case

$$\ell_\gamma = c\tau \gg \ell_e ,\ 2\beta_\gamma\sqrt{1+r_e^2/a_\gamma^2} \qquad (19a)$$

and the result can be obtained from (18b - d) by simple substitution of $F_e(0)$ by $F_\gamma(0)$.

$$J = 2\pi\beta_\gamma F_\gamma(0)\sqrt{1+r_e^2/a_\gamma^2} \qquad (19b)$$

---

* The main contribution to the integral J (16) is given by distances $|z|\lesssim\beta_\gamma\sqrt{1+r_e^2/a_\gamma^2}$ and $|z+ct|\lesssim \ell_\gamma$ smaller than ℓ_e. So, $F_e(z-ct)$ can be replaced by $F_e(0)$, that gives (18b).

$$A_0 = \frac{\hbar c}{2\sigma_c F_\gamma(0)}\sqrt{1+r_e^2/a_\gamma^2} \sim \frac{\hbar c\,\ell_\gamma}{2\sigma_c} = 6.3\,\frac{\sigma_0}{\sigma_c}\,\ell_\gamma(cm)\ J. \qquad (19c)$$

The important distinction from the previous case consists in the fact that here all the electrons effectively take part in the conversion, i.e. approximation (15) is valid up to $k\sim 1$.

Note that in this case the conversion coefficient is defined, in fact, by the laser power $P=A/\tau$:

$$k=\frac{P}{P_0},\quad P_0=\frac{A_0}{\tau}\sim\frac{\hbar c^2}{2\sigma_c} = 2\cdot 10^{11}\, W\,\frac{\sigma_0}{\sigma_c} \qquad (19d)$$

One can show that if condition (19a) is not fulfilled, the laser power P_0 necessary for obtaining $k\sim 1$ is only larger than (19d).

5.5. Intermediate cases

In intermediate cases result depends on the linear densities $F_e(z)$ and $F_\gamma(z)$ of electrons and photons along the beam direction. For example, in the case when both bunches are long and their lengths are of the same order $(\ell_e\sim\ell_\gamma\gg\beta_\gamma\sqrt{1+r_e^2/a_\gamma^2})$ it is easy to get

$$J = 2\pi\beta_\gamma\sqrt{1+r_e^2/a_\gamma^2}\int F_e(z)F_\gamma(-z)\,dz \qquad (20)$$

Let us consider two simple models.

In the first one both distributions are uniform:

$$F_e(z)=\frac{1}{\ell_e}\quad at\ |z|\le\frac{\ell_e}{2},\qquad F_\gamma(z)=\frac{1}{\ell_\gamma}\quad at\ |z|\le\frac{\ell_\gamma}{2}. \qquad (21a)$$

After substitution of these functions in (16), one obtains:

$$J=\frac{2}{\delta_1^2-\delta_2^2}\left[\delta_1\arctan\delta_1-\delta_2\arctan\delta_2-\frac{1}{2}\ln\frac{1+\delta_1^2}{1+\delta_2^2}\right],\ \delta_{1,2}=\frac{|\ell_e\pm\ell_\gamma|}{4\beta_\gamma\sqrt{1+r_e^2/a_\gamma^2}}. \qquad (21b)$$

In the other model both distributions have Gaussian shape

$$F_e(z)=\sqrt{\frac{2}{\pi}}\frac{1}{\ell_e}\exp\left(-\frac{2z^2}{\ell_e^2}\right),\quad F_\gamma(z)=\sqrt{\frac{2}{\pi}}\frac{1}{\ell_\gamma}\exp\left(-\frac{2z^2}{\ell_\gamma^2}\right) \qquad (22a)$$

In this model

$$J(\delta)=\frac{2}{\sqrt{\pi}}\int_0^\infty \frac{e^{-x^2}dx}{1+\delta^2x^2}, \quad \delta=\sqrt{\delta_1^2+\delta_2^2}=\frac{\sqrt{2(l_e^2+l_\gamma^2)}}{4\beta_\gamma\sqrt{1+r_e^2/a_\gamma^2}}. \tag{22b}$$

The graph of the function $J(\delta)$ (22b) is given in fig. 4.

A numerical investigation of J (21b),(22b) shows the following: the approximation of short bunches (17) is good up to $\delta \approx 1$ (in both models $J > 0.75$ at $\delta < 1$). The long bunch approximation is well suited only at sufficiently large δ-values. The deviation of J from asymptotic formulae is less than 20% at $\delta \gtrsim 10$ only. For all δ-values J are smaller than their asymptotical values corresponding to (18),(19).

5.6. The minimal value of A_o

The minimal A_o value is obtained in the case when a radius r_e of an electron beam is small, and photon bunch sizes are small as well. This variant was considered in ref. [15]. In this case the long bunch approximation (18),(19) is valid and the result depends on the electron bunch length l_e only

$$A_o=\frac{\hbar c}{2\sigma_c F_e(0)} \sim \frac{\hbar c l_e}{2\sigma_c} = 6.3\,\frac{\sigma_o}{\sigma_c}\,l_e(cm)\ J. \tag{23a}$$

This estimation for A_o is valid only under the conditions (taking into account (18),(14)):

$$l_\gamma = c\tau < l_e, \quad r_e < a_\gamma < \sqrt{\lambda l_e/80\pi}. \tag{23b}$$

5.7. Beam collision angle $\alpha_o \neq 0$

All the previous calculations were carried out for a head-on collision, $\alpha_o = 0$. This can be realized using spherical mirror or lense with a hole for electron beams. It can occur that for some technical reason $\alpha_o \neq 0$ is more convenient. Let us discuss briefly how k depends on α_o (at $\alpha_o \ll 1$).

For short bunches at $\alpha_o < max(a_\gamma/l_\gamma, r_e/l_e)$ the conversion coefficient practically does not differ from eqs. (17).

In the long bunch case the simple calculation similar to

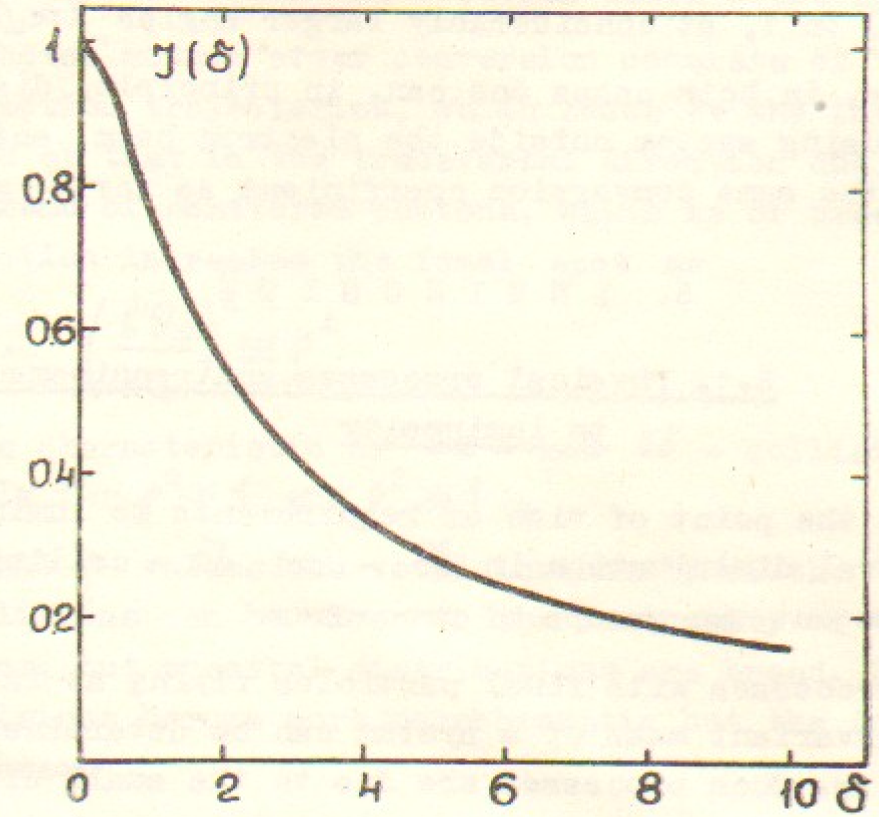

Fig. 4. Function $J(\delta)$ (22).

that giving (16) leads to appearance in A_0 (18),(19) of the additional factor χ , where

$$\chi = \frac{e^t}{I_0(t)}\ , \quad t = \frac{\alpha_0^2}{2\alpha_\gamma^2} \qquad (24)$$

(here $\alpha_\gamma = a_\gamma/\beta_\gamma$ is an angular size of the laser beam, $I_0(t)$ is the Bessel function for imaginary argument). At $\alpha_0 \lesssim \alpha_\gamma$ the value of $\chi \approx 1$, at considerably larger angles $\chi \approx \sqrt{\pi}\,\alpha_0/\alpha_\gamma$.

Hence, in both cases one can, in principle, dispose the laser focusing system outside the electron beam, and get approximately the same conversion coefficient as for $\alpha_0 = 0$.

6. L U M I N O S I T Y

6.1. Physical processes and requirement to luminosity

From the point of view of requirements to luminosity and its spectral distribution in $\gamma\gamma$ - and γe - collisions one can single out two groups of processes:

a) Processes with final particles flying at large angles, so that invariant mass of a system can be determined by reaction products. Such processes are due to the small distance interaction. Their cross sections are small enough $\sim (\alpha\hbar/m_W c)^2 \div (\alpha\hbar c/E)^2 \sim 10^{-34} \div 10^{-36}$ cm^2 and smoothly depend on the energy (excluding the threshold region). For their investigation the maximal available luminosity is necessary but not monochromatization.

b) Processes for which a sufficiently good monochromatization is useful. Such are, e.g., processes due to interaction at large distances. Their cross sections are large, but drop rapidly with the growth of transverse momenta of particles. The detection of all reaction products flying at small angles is a very difficult task. Therefore, here monochromatic collisions are very useful, but not high luminosity. Another example is a new particle production with evident threshold or resonant behaviour. For example, the $\gamma\gamma \to W^+W^-$ cross section increases up to the half of its asymptotic value in the energy range 10% above threshold.

6.2. Qualitative consideration

The luminosity of $\gamma\gamma$ - and γe - collisions is defined by a number of particles and beam sizes in the interaction region. The length of the γ - bunch coincides with the length of the electron bunch ℓ_e *. Its size in the interaction region is larger than that which the electron bunch could have.

The photon motion after conversion consists of that along initial electron trajectories, which focus at the interaction region, and of that in the transversal direction due to the angular spread of scattered photons, which is of order of θ_0. The last motion increases the focal spot as

$$\frac{\Delta S_{eff}}{S_{eff}} \sim \left(\frac{b\theta_0}{a_e}\right)^2 \equiv \rho^2. \qquad (25)$$

Qualitative characteristic of γe - and $\gamma\gamma$ - collisions differ considerably for $\rho^2 \ll 1$ and $\rho^2 \gg 1$.

At small ρ values the total luminosity of the γe - and $\gamma\gamma$ - collisions can be close to the luminosity of the e^+e^- - collisions, but spectral distributions are broad. For large ρ, collisions become more monochromatic but the total luminosity decreases.

Below in this section only the case $\rho^2 \ll 1$ is considered.

6.3. The total luminosity

As $\rho^2 \ll 1$, then in the interaction region the γ - bunch has the same transversal size, length and β - function as the electron bunch could have had. Therefore, the total luminosities of the γe - and $\gamma\gamma$ - collisions are equal to

$$L_{\gamma e} = k L_{ee}\ , \quad L_{\gamma\gamma} = k^2 L_{ee} \qquad (26)$$

where L_{ee} is the luminosity which e^+e^- - collisions could have had without taking into account charged beam collision effects in the interaction region. If the electron bunches are short, $\ell_e < 2\beta_e$, as it takes place for accelerators considered, then

* Excluding the case $\ell_e > 2\beta_\gamma, c\tau$, when length of the γ -bunch is less than ℓ_e.

$$L_{ee} = \nu \frac{N_{e^+} N_{e^-}}{2\pi a_e^2} \qquad (27)$$

6.4. Spectral luminosity

The number of scattered photons with the energy in the range from ω to $\omega + d\omega$ is (cf.(5),(6))

$$dN_\gamma = N_e \frac{k}{\sigma_c} \frac{d\sigma_c}{d\omega} d\omega = k N_e f(x, \frac{\omega}{E}) \frac{d\omega}{E}. \qquad (28)$$

Substituting dN_γ for N_{e^+} into (27),(26) one finds luminosity distribution in γe - collisions over the γe - invariant mass $W_{\gamma e} = \sqrt{4\omega E}$.

$$\frac{dL_{\gamma e}}{dz} = 2zkL_{ee}\, f(x, z^2), \quad z = \frac{W_{\gamma e}}{2E} = \sqrt{\frac{\omega}{E}}. \qquad (29)$$

This function is shown in fig. 6 (the curve for $\rho = 0$). Let us note that the luminosity is concentrated in the region of large $W_{\gamma e}$. For the laser (3) and $E = 50 \div 300$ GeV the range $W_{\gamma e} > \frac{1}{2}(W_{\gamma e})_{max}$ contains 70 ÷ 80 % of the total luminosity.

Similar calculations for $\gamma\gamma$ - collisions give us

$$dL_{\gamma\gamma} = k^2 L_{ee}\, f(x, \frac{\omega_1}{E}) f(x, \frac{\omega_2}{E}) \frac{d\omega_1}{E} \frac{d\omega_2}{E}. \qquad (30a)$$

From here the luminosity distribution over $\gamma\gamma$ - invariant mass $W_{\gamma\gamma} = \sqrt{4\omega_1\omega_2}$ is

$$\frac{dL_{\gamma\gamma}}{dz} = 2zk^2 L_{ee} \int_{z^2/y_m}^{y_m} f(x,y)\, f(x, \frac{z^2}{y}) \frac{dy}{y}, \quad z = \frac{W_{\gamma\gamma}}{2E}. \qquad (30b)$$

Graphs of this functions for various x are given in fig. 5. In the whole x - range under consideration the luminosity distribution over $W_{\gamma\gamma}$ is very broad.

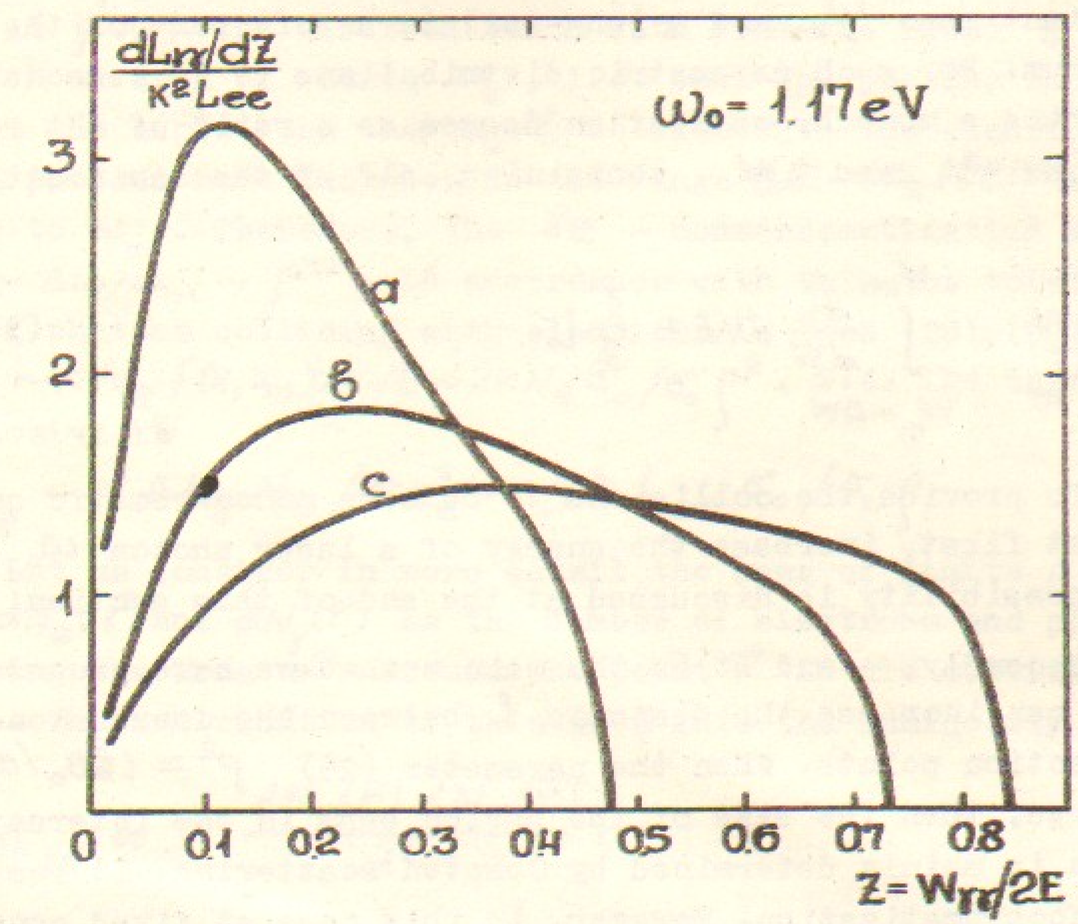

Fig.5. Spectral luminosity of the $\gamma\gamma$ -collisions at $\rho^2 = (b\theta_o/a_e)^2 \ll 1$. Curves a, b and c correspond to E=50, 150 and 300 GeV.

7. MONOCHROMATIZATION

7.1. Definition, different variants

In the considered below methods of the luminosity monochromatization, the distribution dL/dW both for γe - and $\gamma\gamma$ - collisions has a maximum near the maximal value of the invariant mass W_m and a long tail in a soft part of the spectrum. For such asymmetric distributions it is reasonable to define a monochromatization degree as a ratio of the range of invariant mass ΔW, containing half of the luminosity, to W_m:

$$\eta = \frac{\Delta W}{W_m}, \quad \int\limits_{W_m-\Delta W}^{W_m} \frac{dL}{dW}\, dW = \frac{1}{2} L . \tag{31}$$

To provide the collisions to be more monochromatic one can, at first, increase the energy of a laser photon ω_0. This possibility is discussed at the end of this section.

Secondly, - and it is the main method we have proposed - - one can increase the distance b between the conversion and interaction points. When the parameter (25) $\rho^2 = (b\theta_0/a_e)^2 \gg 1$ is large, then the size of the photon beam in the interaction region is mainly determined by Compton scattering. It results in monochromatization. However, in this case at fixed conversion coefficient the necessary laser flash energy (17) grows as b^2 since the electron bunch radius in the conversion region is proportional to b (9) (the laser bunch radius should be increased accordingly).*)

We assume below the electron bunch to be short ($l_e < 2\beta_e$). Besides, in our calculations the finite lengths of the conversion region $l_{conv} \sim \min\{2\beta_\gamma, (l_e+l_\gamma)/2\}$ and of the interaction region $l_{int} \sim l_e/2$ are not taken into account. The detailed calculations show us that the account of these finite lengths leads both for γe - and $\gamma\gamma$ - collisions to the small relative variance of luminosities and monochromatization degrees

*) Considerably better monochromatization is obtained at the scattering of polarized laser light on the polarized electrons - see a forthcoming paper.

$$\frac{\Delta L_{\gamma e}}{L_{\gamma e}} \sim \frac{\Delta L_{\gamma\gamma}}{L_{\gamma\gamma}} \sim \frac{\Delta\eta}{\eta} \sim \left(\frac{l_{conv}+l_{int}}{2b}\right)^2 . \tag{32}$$

7.2. γe - collisions

At $\rho^2 \gg 1$ the electron bunch cuts from the broad γ - - bunch an area of radius a_e, i.e. only the photons scattered at the angle less than a_e/b collide with the electrons. These photons have energies in the range $\Delta\omega \sim (a_e/b\theta_0)^2\omega_m$ (7) close to ω_m. Therefore, the γe - monochromatization degree $\eta_{\gamma e} \sim \Delta\omega/\omega_m \sim \rho^{-2}$. In accordance with this the total number of photons colliding with electrons is (see (28),(6)) $\Delta N_\gamma \sim k N_e f(x, y_m)\Delta\omega/E \sim 2kN_e\sigma_0/\sigma_c\,\rho^2$, i.e. the total luminosity is

$$L_{\gamma e} \sim \nu\,\Delta N_\gamma N_e/\pi a_e^2 \sim 4k\,L_{ee}\,\sigma_0/\sigma_c\,\rho^2 .$$

Let us consider in more detail the case of finite ρ. Let $dN_e(\vec r)$ and $dN_\gamma(\vec r)$ be the number of electrons and photons, crossing the area d^2r around the point $\vec r$ in the collision plane. The contribution of this area into the luminosity equals

$$dL_{\gamma e} = \nu\,\frac{dN_\gamma(\vec r)\,dN_e(\vec r)}{d^2r} . \tag{33}$$

The electron beam in the interaction region is described by the relation (cf.(10))

$$dN_e(\vec r) = \frac{N_e}{\pi a_e^2}\, e^{-r^2/r_e^2}\, d^2r . \tag{10a}$$

To describe the γ-beam it is necessary to consider the photon motion from the conversion region taking into account the distribution of the electrons in this region over their directions and distances from the axis. The photon with the energy ω was radiated at the angle $\theta = \theta_0\sqrt{(\omega_m/\omega)-1}$ to the initial direction of the electron momentum. Taking this into account and averaging over the electron angular distributions, one obtains the simple expression

$$dN_\gamma(\vec{r},\omega)=\int_0^{2\pi}\frac{d\varphi}{2\pi}\,dN_e(\vec{r}-b\vec{\theta})\,\frac{k}{\sigma_c}\,\frac{d\sigma_c}{d\omega}\,d\omega$$

$$\vec{\theta}=\theta_0\sqrt{(\omega_m/\omega)-1}\,(\cos\varphi,\ \sin\varphi). \qquad (34)$$

Substituting (10a), (34) into (33) and integrating over $\vec{r}$ and φ one obtains

$$dL_{\gamma e}=L_{ee}\,\frac{k}{\sigma_c}\,\frac{d\sigma_c}{d\omega}\exp\left[-\left(\frac{\omega_m}{\omega}-1\right)\frac{\rho^2}{2}\right]d\omega,\quad \rho=\frac{b\theta_0}{a_e}. \qquad (35)$$

Hence, it is easy to get the luminosity distribution over $W_{\gamma e}=\sqrt{4\omega E}$

$$\frac{dL_{\gamma e}}{dz}=2zkL_{ee}\,f(x,z^2)\exp\left\{-\left[\frac{x}{(x+1)z^2}-1\right]\frac{\rho^2}{2}\right\},\quad z=\frac{W_{\gamma e}}{2E} \qquad (36)$$

and the total luminosity

$$L_{\gamma e}=kL_{ee}\int_0^{y_m}f(x,y)\exp\left[-\left(\frac{y_m}{y}-1\right)\frac{\rho^2}{2}\right]dy \qquad (37)$$

(the function $f(x,y)$ is defined in (6)).

At $\rho\to 0$ one can obtain from here the known results (26), (29).

Graphs of the spectral and total luminosity and the monochromatization degree $\eta_{\gamma e}$ (31) are presented in figs. 6,7. It is seen that with the ρ- growth the decrease of the total luminosity is due to diminishing of the spectral luminosity in the soft part of the spectrum only.

With the ρ - increase at fixed x the monochromatization improves quickly. E.g., for x = 2.69 and ρ^2 = 10 the monochromatization degree $\eta_{\gamma e}$ = 3.4% is close to that of the initial electrons beams $\Delta E/E\sim 1\%$. The corresponding luminosity $L_{\gamma e}$ = 0.21 L_{ee} , i.e. it can be large enough.

At $\rho\to\infty$ from (36),(37) and (8a) it is easy to obtain the asymptotic formulae (in accordance with the above estimations)

$$L_{\gamma e}=\frac{kL_{ee}}{\rho^2}\,\frac{4\sigma_0}{\sigma_c}\left[1+\frac{1}{(x+1)^2}\right]\left(1-\frac{2D}{\rho^2}+\ldots\right)$$

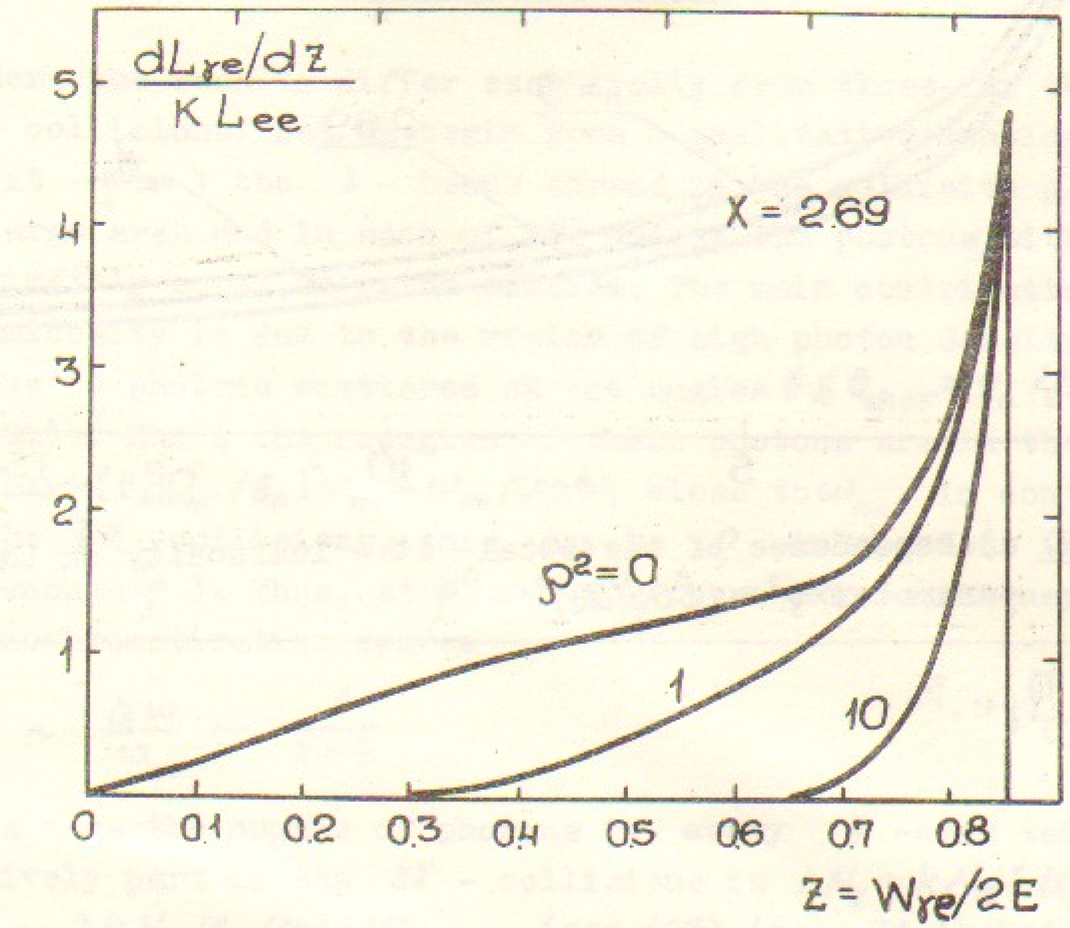

Fig.6. Spectral luminosity of the γe -collisions (36) for x=2.69 (E=50 GeV, ω_0 = 3.5 eV or E=150 GeV, ω_0 =1.17 eV) at different $\rho^2=(b\theta_0/a_e)^2$

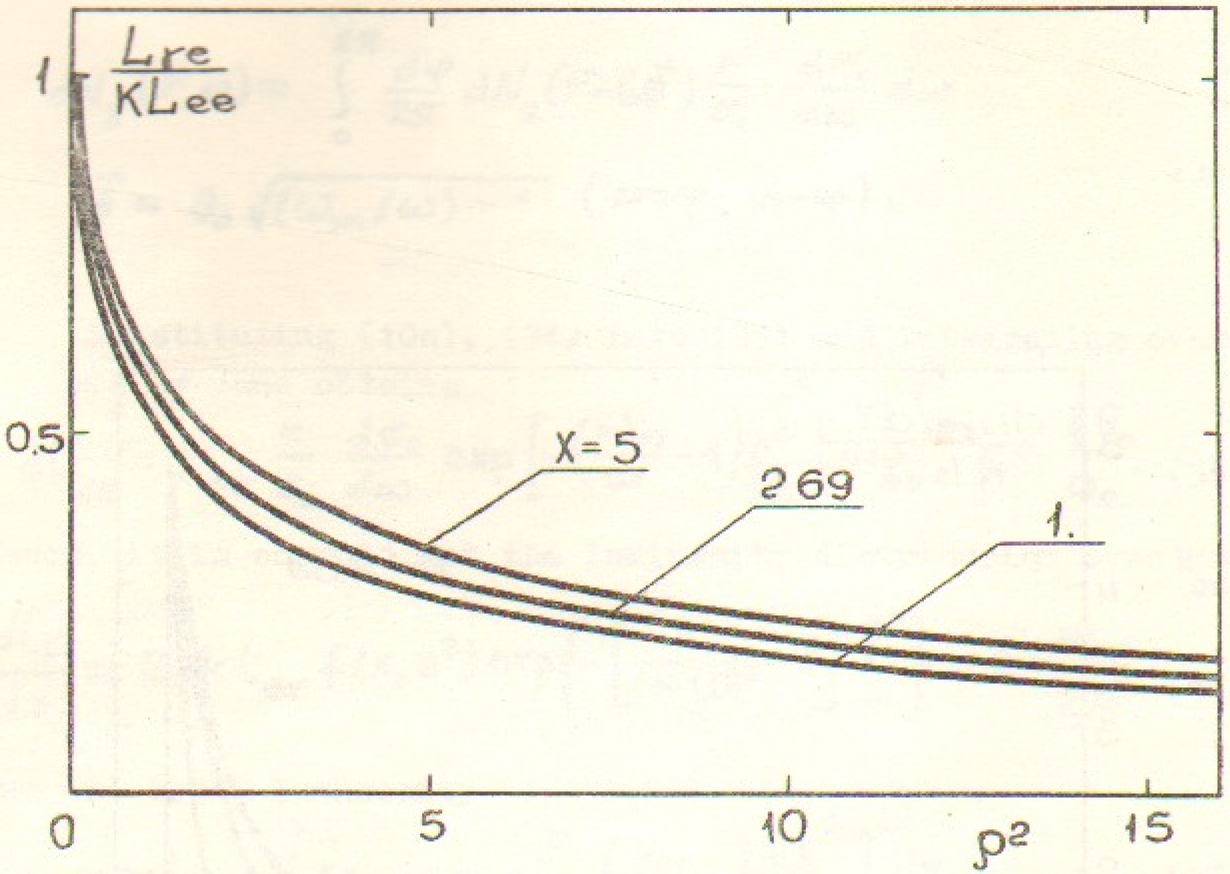

Fig.7. a) Dependence of the total γe - luminosity on the parameter $\rho^2 = (b\theta_0/a_e)^2$

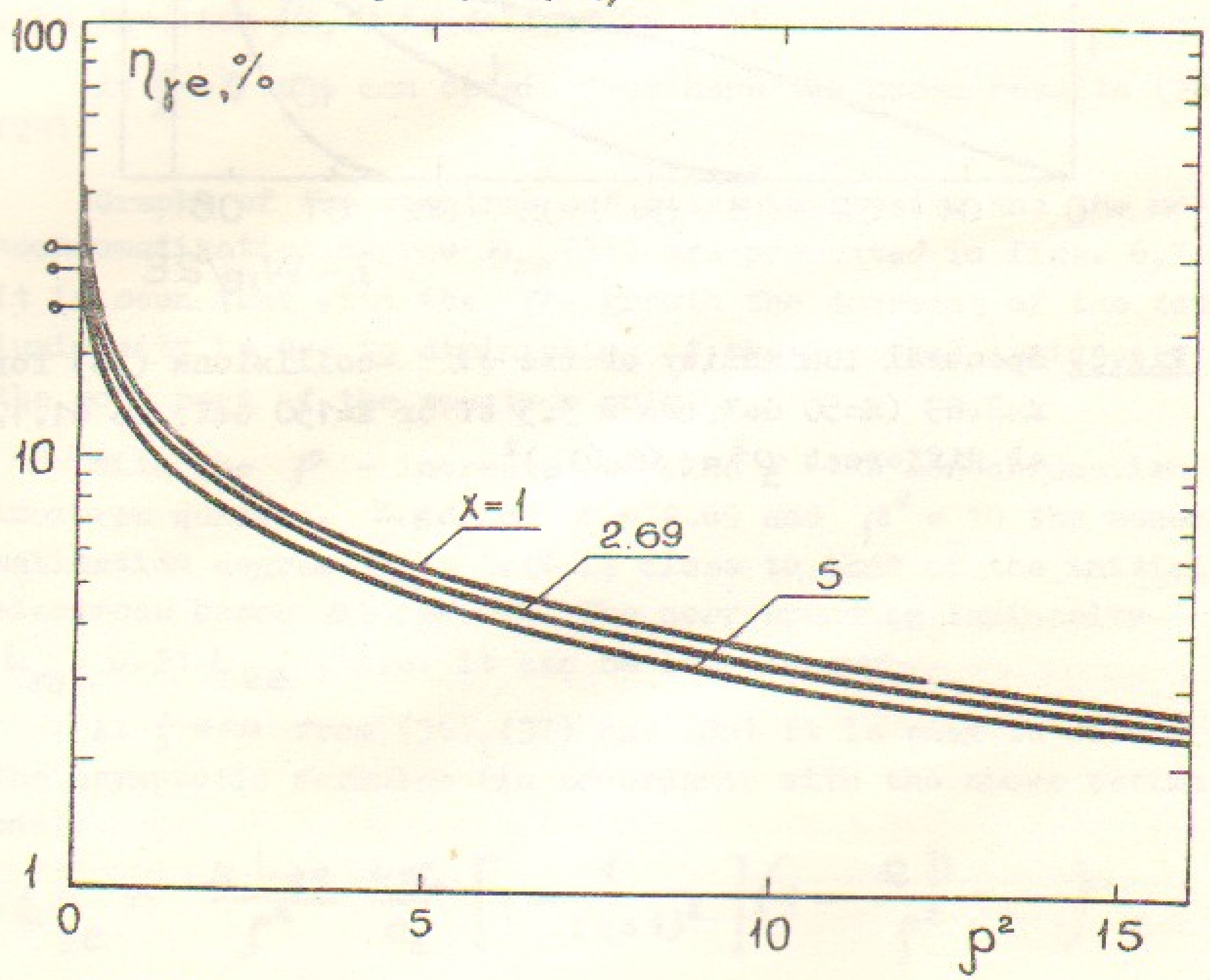

Fig.7b) Dependence of the monochromatization degree for the γe - collisions on ρ^2.

$$\eta_{\gamma e} = \frac{\ln 2}{\rho^2}\left[1 - \frac{2D + (3/2)\ln 2}{\rho^2} + \dots\right], \quad D \approx x+6. \qquad (38)$$

These asymptotics are valid only at $\rho^2 \gg x+6$.

7.3. $\gamma\gamma$ - collisions

Here the results differ essentially from those for the γe - collisions. Let us begin from a qualitative consideration. At $\rho^2 \gg 1$ the γ - beams spread in the collision plane on a large area and in each of its points the photons with the approximately equal energies collide. The main contribution to the luminosity is due to the region of high photon density, i.e. due to photons scattered at the angles $\theta \lesssim \theta_{char} = \theta_0/\sqrt{x+6}$ (see (8a)). Hence the energies of these photons are in the range $\Delta\omega \sim (\theta_{char}/\theta_0)^2\omega_m = \omega_m/(x+6)$, close to ω_m. In contrast with the γe -collisions, this $\Delta\omega$ is ρ -independent (at large enough ρ). Thus, at $\rho^2 \gg x+6$ there exists the asymptotic monochromatization degree

$$\eta^{as}_{\gamma\gamma} \sim \frac{\Delta\omega}{\omega_m} \sim \frac{1}{x+6} \qquad (39a)$$

In this case the number of photons in every γ -beam taking effectively part in the $\gamma\gamma$ - collisions is $\Delta N_\gamma \sim kN_e f(x, y_m) \cdot \Delta\omega/E \sim 2kN_e\sigma_0/(x+6)\sigma_c$ (see (28),(6)). It is interesting to note that in the wide range of values $x = 1 \div 20$ this number is practically x -independent, $\approx 0.2kN_e$. Therefore, the total luminosity in this range is

$$L^{as}_{\gamma\gamma} \sim \nu\frac{(\Delta N_\gamma)^2}{\pi(b\theta_{char})^2} \sim 0.1\,(x+6)\,\frac{kL_{ee}}{\rho^2}. \qquad (39b)$$

If ρ^2 is not too large, one has to take into account the influence of the transversal electron beam size. That gives a spread of the photon energy in every collision point $\Delta\omega/\omega \sim \sim (a_e/b\theta_0)^2 = \rho^{-2}$. Therefore, the asymptotic monochromatization $\eta^{as}_{\gamma\gamma}$ (39a) is achieved at $\rho^2 \gg x+6$ only.

Let us go from estimations to calculation. By repeating the calculations of subsect. 7.2 and using for both beams expression (34) we obtain for the spectral luminosity

$$dL_{\gamma\gamma} = \frac{k^2 L_{ee}}{\sigma_c^2} \frac{d\sigma_c}{d\omega_1} \frac{d\sigma_c}{d\omega_2} I_0\left(\rho^2\sqrt{\left(\frac{\omega_m}{\omega_1}-1\right)\left(\frac{\omega_m}{\omega_2}-1\right)}\right) \cdot \exp\left[-\left(\frac{\omega_m}{\omega_1}+\frac{\omega_m}{\omega_2}-2\right)\frac{\rho^2}{2}\right] d\omega_1 d\omega_2 \quad (40)$$

where $I_0(x)$ is the Bessel function for imaginary argument. From here, the luminosity distribution over the $\gamma\gamma$- invariant mass $W_{\gamma\gamma} = \sqrt{4\omega_1\omega_2}$ has a form

$$\frac{dL_{\gamma\gamma}}{dz} = 2zk^2 L_{ee} \int_{z^2/y_m}^{y_m} f(x,y) f\left(x,\frac{z^2}{y}\right) I_0\left(\rho^2\sqrt{\left(\frac{y_m}{y}-1\right)\left(\frac{y_m y}{z^2}-1\right)}\right) \cdot \exp\left[-\left(\frac{y_m}{y}+\frac{y_m y}{z^2}-2\right)\frac{\rho^2}{2}\right]\frac{dy}{y}, \quad z = \frac{W_{\gamma\gamma}}{2E} \le \frac{x}{x+1} \quad (41)$$

and the total luminosity is

$$L_{\gamma\gamma} = k^2 L_{ee} \int_0^{y_m} f(x,y_1) f(x,y_2) \cdot I_0\left(\rho^2\sqrt{\left(\frac{y_m}{y_1}-1\right)\left(\frac{y_m}{y_2}-1\right)}\right) \exp\left[-\left(\frac{y_m}{y_1}+\frac{y_m}{y_2}-2\right)\frac{\rho^2}{2}\right] dy_1 dy_2 \quad (42)$$

At $\rho \to 0$ the know results (26),(30) can be obtained from (41),(42).

Graphs of the spectral and total luminosity as well as the monochromatization degree $\eta_{\gamma\gamma}$ (31) depending on ρ are presented in figs. 8,9. It is seen that with ρ-growth the soft part of the spectrum decreases faster than the hard one. Just for this reason the monochromatization improves rapidly up to $\rho^2 \sim x+6$. At this value for all curves in fig. 9*

$$L_{\gamma\gamma} \approx 0.07 k^2 L_{ee}, \quad \eta_{\gamma\gamma} \approx 1.5\eta_{\gamma\gamma}^{as}, \quad (\rho^2 = 1/\eta_{\gamma\gamma}^{as}). \quad (43)$$

At the further ρ growth the luminosity decreases rapidly (as ρ^{-2}) and the monocromatization degree decreases very slowly, approaching to $\eta_{\gamma\gamma}^{as}$, the spectral luminosity tends to the function

* In the interval $\eta_{\gamma\gamma} W_m$ near W_m the integral of luminosity is $\approx 0.035\, k^2 L_{ee}$. (At $\rho^2 \ll 1$ such integral in the same range is $\approx 0.065\, k^2 L_{ee}$).

The numerical analysis shows us that at $\rho^2 \gtrsim x+6$ the maxima of all $dL_{\gamma\gamma}/dW_{\gamma\gamma}$ curves are at $W_{\gamma\gamma} \approx W_m - (\eta_{\gamma\gamma} - \eta_{\gamma\gamma}^{as})W_m$.

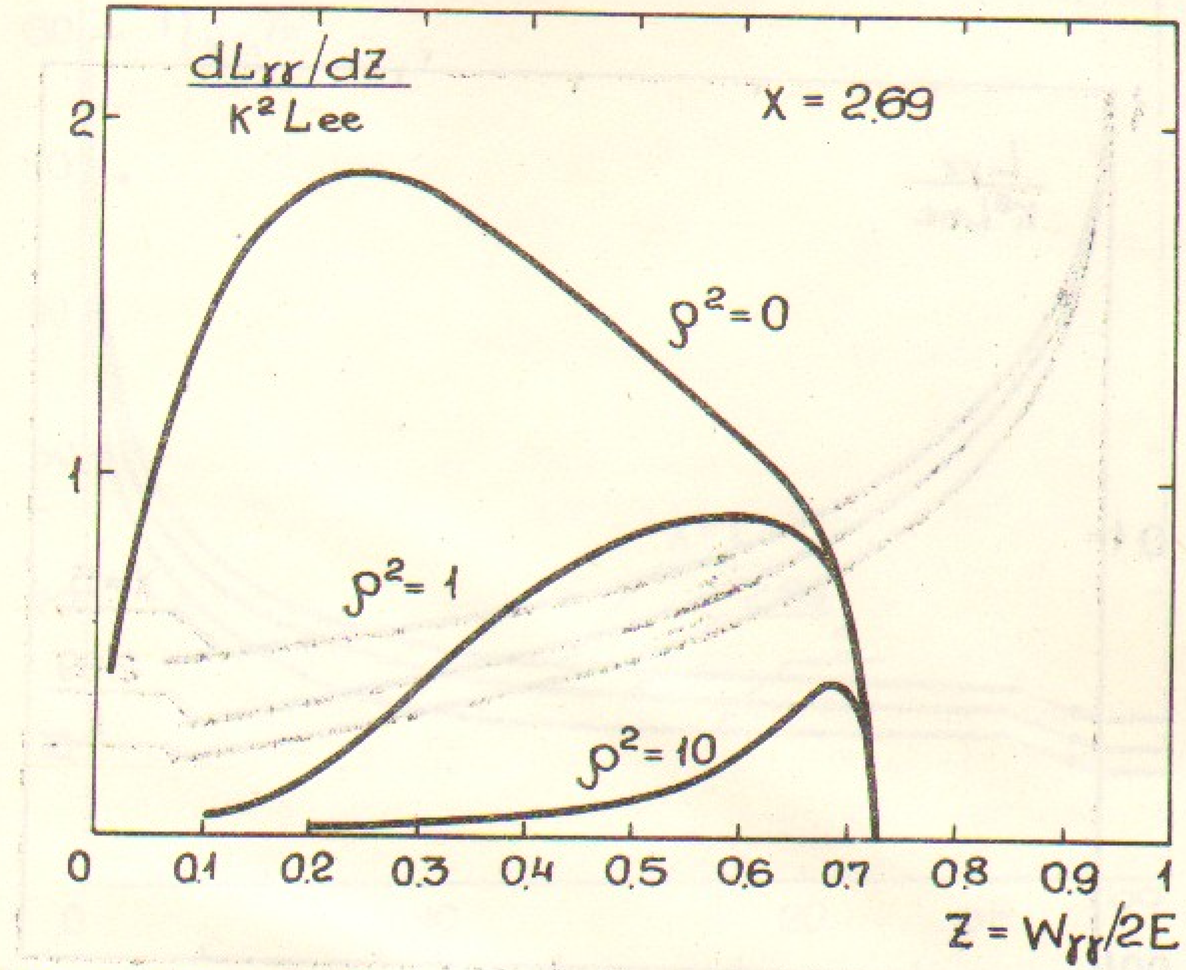

Fig.8. Spectral luminosity of the $\gamma\gamma$ -collisions (41) for $x=2.69$ (E=50 GeV, ω_0 = 3.5 eV or E=150 GeV, ω_0=1.17 eV) at different $\rho^2 = (b\theta_0/a_e)^2$

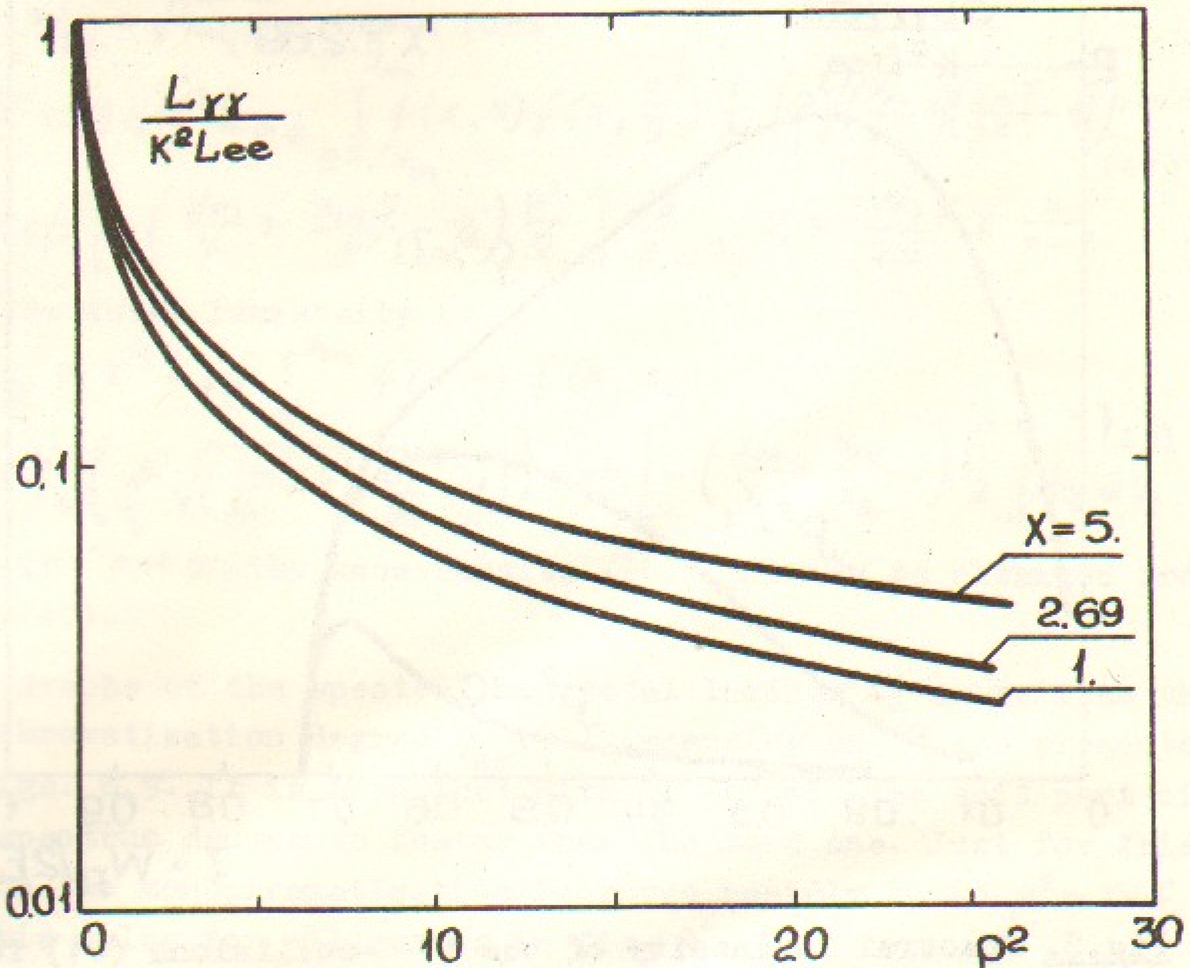

Fig.9. a) Dependence of the total $\gamma\gamma$ -luminosity on the parameter $\rho^2 = (b\theta_0/a_e)^2$

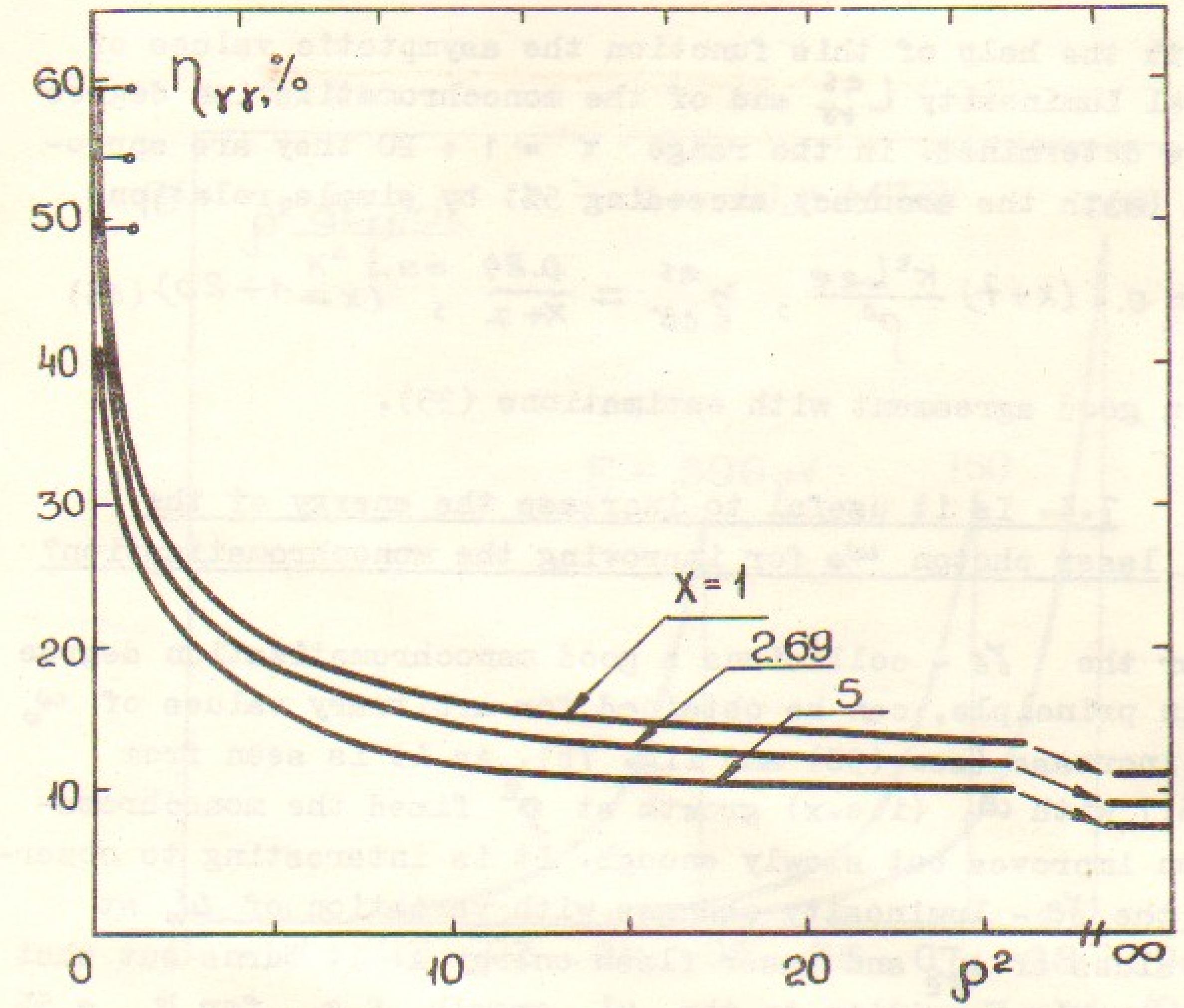

Fig. 9 b) Dependence of the monochromatization degree for the $\gamma\gamma$ -collisions on ρ^2 .

$$\frac{dL^{as}_{\gamma\gamma}}{dz} = \frac{2k^2 L_{ee}}{\rho^2 y_m}\left[z f(x,z)\right]^2. \qquad (44)$$

Graphs of this function are shown in fig. 10.

With the help of this function the asymptotic values of the total luminosity $L^{as}_{\gamma\gamma}$ and of the monochromatization degree $\eta^{as}_{\gamma\gamma}$ are determined. In the range $x = 1 \div 20$ they are approximated (with the accuracy exceeding 5%) by simple relations

$$L^{as}_{\gamma\gamma} = 0.1\,(x+7)\frac{k^2 L_{ee}}{\rho^2}, \quad \eta^{as}_{\gamma\gamma} = \frac{0.84}{x+7}, \quad (x = 1 \div 20) \qquad (45)$$

It is in good agreement with estimations (39).

7.4. Is it useful to increase the energy of the laser photon ω_0 for improving the monochromatization?

For the γe - collisions a good monochromatization degree $\eta_{\gamma e}$, in principle, can be obtained for arbitrary values of ω_0 by ρ increase (see (38) and fig. 7b). As it is seen from figs. 6,7 with ω_0 (i.e.x) growth at ρ^2 fixed the monochromatization improves but slowly enough. It is interesting to observe how the γe - luminosity changes with variation of ω_0 at fixed values of $\eta_{\gamma e}$ and laser flash energy A. It turns out that $L_{\gamma e}$ is weakly sensitive to the ω_0 -growth. E.g., for $\eta_{\gamma e} = 5\%$ the variation of ω_0 resulting from x variation from 1 up 10, the luminosity decreases by factor 1.5. This conclusion can also be obtained from asymptotic eqs.(38) which give, with the account of (7), (17b), $L_{\gamma e} \propto A(1+x^{-1})\,\eta_{\gamma e}$ (here the fact that $A_0 = \pi(r_e^2 + a_\gamma^2)\,\omega_0/\sigma_c \propto x\rho^2/(x+1)\sigma_c$ is taken into account).

For $\gamma\gamma$-collisions there is the asymptotic monochromatization degree $\eta^{as}_{\gamma\gamma}$ (45) which is weakly ω_0 dependent. E.g., $\eta^{as}_{\gamma\gamma}$ changes only two times when x grows from 1 to 10. At the same time the luminosity at fixed A decreases by factor ~ 100 (since $L^{as}_{\gamma\gamma} \propto [(x+1)(\ln x + 0.5)/x^2(x+7)]^2$).

Therefore, the increase of ω_0 does not improve considerably the monochromatization, but requires the increase of the la-

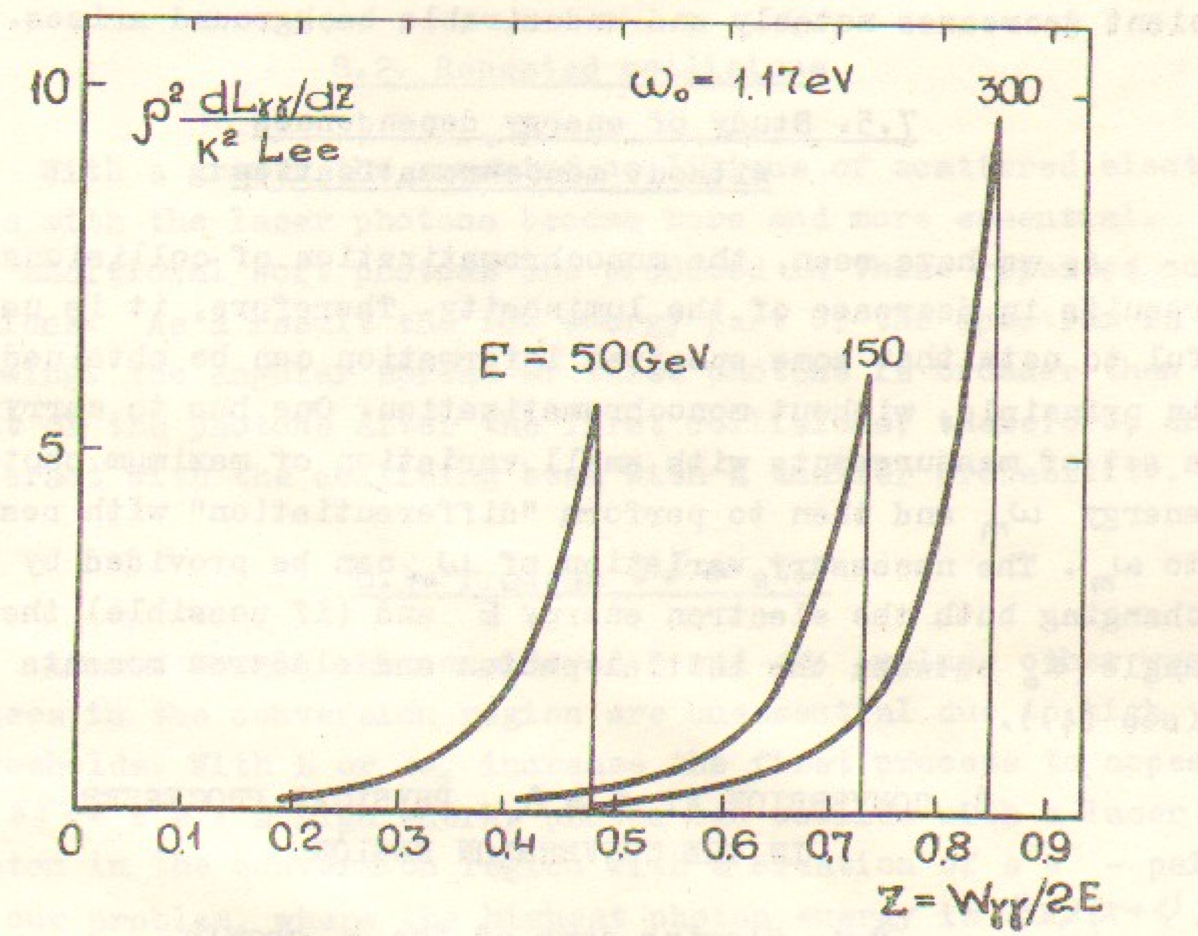

Fig.10. Spectral luminosity of the $\gamma\gamma$ -collisions (44) at $\rho^2 = (b\theta_0/a_e)^2 \gg x+6$.

ser flash energy for keeping the luminosity. In addition, at $x > 4.8$ the production of the e^+e^- - pairs in the collisions of high energy photons with the laser photons becomes essential (this process is discussed in sect. 8 and Appendix B). This process results in the decrease of the number of high energy photons. At $x \lesssim 9$, their energy spectrum becomes smoother than fig. 3 shows; at $x > 9$, the hard part of the spectrum becomes sharper, but in both cases the conversion coefficient decreases notably and undesirable background arises.

7.5. Study of energy dependences without monochromatization

As we have seen, the monochromatization of collisions results in decrease of the luminosity. Therefore, it is useful to note that some spectral information can be obtained, in principle, without monochromatization. One has to carry out a set of measurements with small variation of maximum photon energy ω_m and then to perform "differentiation" with respect to ω_m. The necessary variation of ω_m can be provided by changing both the electron energy E and (if possible) the angle α_o between the initial photon and electron momenta (see (4)).

8. CONVERSION AT $A \gtrsim A_o$. PHYSICAL PROCESSES IN THE CONVERSION REGION

8.1. Slowing down of the k growth

The formulae of sect. 5 are valid when the collision probability for any electron is small, i.e. at $A \ll A_o$, with A growth at $A \gtrsim A_o$ the conversion coefficient increases slower than that predicted by simple linear relation $k = A/A_o$.

If every electron meets the same number of photons the conversion coefficient would be equal to $k = 1 - \exp(-A/A_o)$. Taking into account beam inhomogeneity modifies this simple result. E.g., in the case of short bunches (17) with the Gaussian distribution of the transversal density the conversion coefficient for every electron depends on distance r from the axis, $k(r) = 1 - \exp[-A/A_o(r)]$. After averaging of this expression with the transversal beam density (10) we obtain

$$k = \mu \int_0^1 [1 - \exp(-\frac{\nu}{\mu} t)]\, t^{\mu-1} dt, \qquad (46)$$

$$\mu = a_\gamma^2 / r_e^2, \quad \nu = A\sigma_c / \pi r_e^2 \omega_o$$

According to this eq., for $\nu = 1$ or 2, the maximum values of $k = 0.4$ (or 0.58) are achieved at $a_\gamma^2 = 0.53\, r_e^2$ (or $0.75\, r_e^2$). (Cf. $k = 0.37$ or $k = 0.51$ at $a_\gamma = r_e$).

8.2. Repeated collisions

With a growth the repeated collisions of scattered electrons with the laser photons become more and more essential. The additional soft photons are produced in these repeated collisions. As a result the low energy part of the spectrum is growing. The angular spread of these photons is broader than that of the photons after the first collisions, therefore, they interact with the colliding beam with a smaller probability.

8.3. Process $\gamma\gamma \to e^+e^-$

Almost in all the considered E and ω_o values other processes in the conversion region are unessential due to high thresholds. With E or ω_o increase the first process to appear is $\gamma\gamma \to e^+e^-$: a high energy photon can collide with a laser photon in the conversion region with a creation of e^+e^- - pair. In our problem, where the highest photon energy is $Ex/(x+1)$, the threshold of this process ($4\omega\omega_o > 4m_e^2c^4$) corresponds to $x > 2(1+\sqrt{2}) \approx 4.8$. For the neodymium glass laser (3) that corresponds to the electron energy $E \approx 270$ GeV.

At small excess over the threshold the cross section of this process (B.5) grows up to $4\omega\omega_o \approx 8m_e^2c^4$, where it is about $0.7\,\sigma_o$. This value of ω is reached firstly at $x \approx 8.9$ (where the Compton cross section is $0.54\sigma_o$). Therefore, at $4.8 < x < 8.9$ the more energetic photons are effectively knocked out from the beam which leads to softening of the spectrum. With x growth from 4.8 to 8.9 at $A \gtrsim A_o$ its role becomes more and more essential.

8.4. Region $x > 8$. Process $\gamma e \to e e^+ e^-$

It is doubtful whether the x values greater than 8 are of real interest in the near future (cf. table 1). However, we would like to discuss here, for completeness, essential features of physical processes in this region.

First of all, at $x > 8.9$ the low energy photons are knocked out from the beam more often than the hard ones due to the process $\gamma\gamma \to e^+e^-$. That leads to sharpening of the spectrum in comparison with this obtained at a single Compton scattering. At $x \gg 9$ the $\gamma\gamma \to e^+e^-$ cross section exceeds that of Compton scattering (5) not less than twice. This leads to essential restriction upon the maximum value of the conversion coefficient for the high energy photons.

Secondly, at $x > 8$ production of the e^+e^- - pairs becomes possible in the collision of an electron with a laser photon ($e\gamma \to ee^+e^-$). For laser (3) this corresponds to $E > 450$ GeV, in the case of frequency tripling - to $E > 150$ GeV. At all moderate values of x the $e\gamma \to ee^+e^-$ cross section is small, $\sim \alpha\sigma_0$, and can be neglected. With the growth of x this cross section increases slowly (B.9) - in contrast with the decrease of the Compton cross section. However, even at $x = 100$ it equals $1/7$ only and the role of this process in the conversion is small enough.

9. MAIN RESULTS FOR THE SLC AND VLEPP

In the tables presented below the examples of the essential quantities are gathered, characterizing the conversion, γe- and $\gamma\gamma$ -collisions for SLC and VLEPP with the use of neodymium (Nd) glass or garnet laser (3) - the most powerful modern solid state laser. Symbol 3 Nd corresponds to laser (3) with the frequency tripling ($\omega_0 = 3.5$ eV or $\lambda = 0.35 \mu m$), which allows one to increase the maximum energy of the scattered photons ω_m. For powerful laser (3) the frequency tripling with efficiency of about 100% is realized in a number of experiments (e.g., in ref. [16] the efficiency is 80% at A=30J).

The presented values of A allow one to determine the conversion due to the known energy of the laser flash A by simple relation (15) $k = A/A_0$ at $A < A_0/2$. At $A > A_0/2$ the efficiency of an additional energy contribution decreases, cf. sect.8.

9.1. Choice of b

The distance b between interaction and conversion regions should be determined by some compromise.

On the one hand, with b increasing the cross section of the electron beam (9) and A_0 are growing as well. The typical b -dependence of A_0 is shown in fig. 11. Moreover, the γ - beam transversal size in the interaction region grows with the growth of b due to angular spread of the scattered photons. This results in decreasing the luminosity even at fixed conversion coefficient.

On the other hand, with b growth, collisions become more and more monochromatic (cf. sect. 7).

At last, one should take into consideration that b should be sufficient to bend electrons from the interaction region by a moderate magnetic field B . On the way b the electron with energy E is shifted across the field B by the distance

$$\Delta = 15 \frac{B(T)\, b^2(cm)}{E(GeV)} \mu m . \qquad (47)$$

For e^+e^- beams the field $\vec{B}$ should change the direction between conversion points, and for e^-e^--beams the field $\vec{B}$ might be uniform.

9.2. Maximum luminosity (without monochromatization)

Table 5 contains the main characteristics for the case of

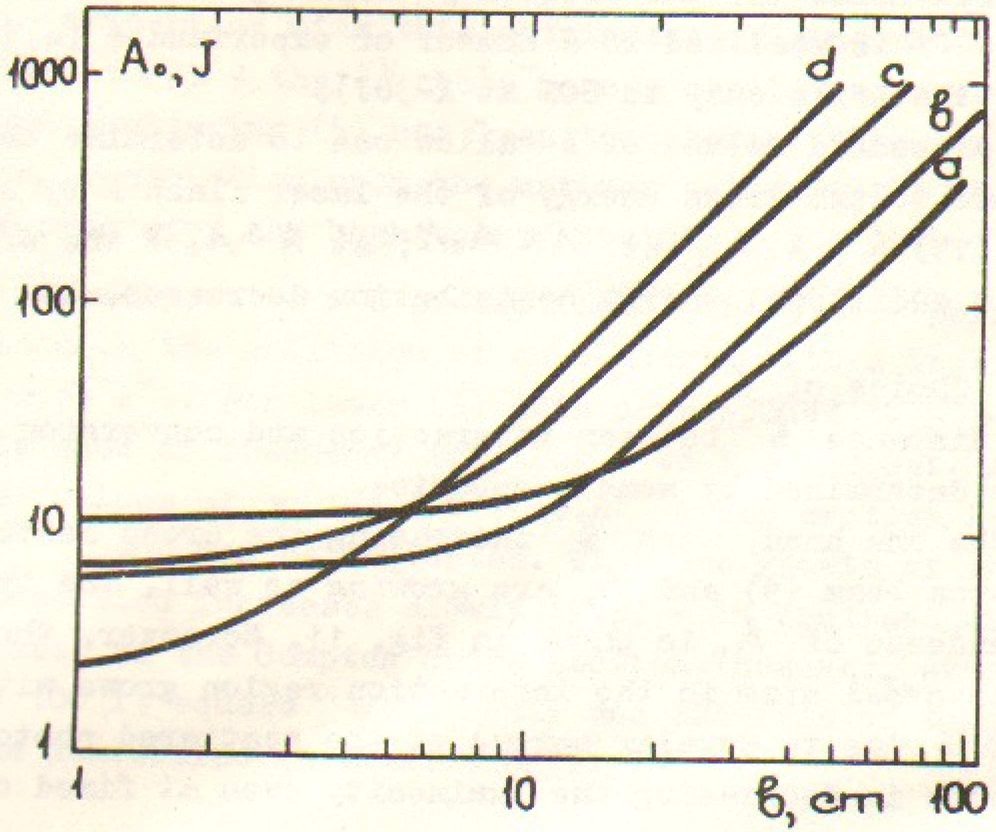

Fig.11. **Dependence of the laser flash energy A_o (22) on the distance between the conversion and collision regions b at $c\tau = l_e$, ω_o = 1.17 eV. Curves:**

a) VLEPP, E=150 GeV, a_γ = 20 μm ;

b) VLEPP, E=150 GeV, $a_\gamma = r_e$;

c) SLC, E=50 GeV, a_γ = 20 μm ;

d) SLC, E= 50 GeV, $a_\gamma = r_e$.

small enough b , when the maximum γe - and $\gamma\gamma$ -luminosity can be obtained. The spectral luminosity is shown in fig. 6 for the γe -collisions (curve at $\rho = 0$) and fig. 5 for the $\gamma\gamma$ -collisions.

At first sight it seems, according to (16), that by decreasing a_γ and r_e one can obtain $A_o = 0$. It is not so. There exists the limiting value A_o (23), only depending on the length of an electron bunch l_e and the value of Compton cross section. These limiting values (0.8 and 2.3 J) are presented in table 5 together with restrictions (23b) (The difference of these A_o values from the minimum values of A_o in fig. 11 is due to the curvers b and d are obtained under additional requirements $l_e = l_\gamma$, $a_\gamma = r_e$). It is seen that in these cases $b < 0.6$ cm or $b < 3$ cm, i.e. to provide the necessary deflection at such small distances is either impossible or very difficult.

The choice b=5 cm for SLC and 10 cm for VLEPP and B = 2T provides good magnetic deflection $\Delta/a_e \gtrsim 8$. This value of deviation is sufficient for the suppression of the "parasite" ee and γe collisions (for details see Appendix B).

We have chosen the focal spot radius $a_\gamma = 20 \mu m$. Such values of a_γ had been obtained in a number of experiments with lasers having the energy A and pulse duration τ of the necessary order of magnitude, see table 4. It occurs in this case that $a_\gamma = r_e$ for SLC and $a_\gamma > r_e = 13 \mu m$ for VLEPP.

Table 4

A, J	14	50	25
τ, ps	140	2000	100
a_γ, μm	17	25	30
reference	[17a]	[17b]	[17c]

At the chosen parameters b , a_γ , r_e and $l_\gamma = c\tau \lesssim l_e$ the short bunch approximation (17) is well suited. With τ growth the energy A_o grows as well, and the result begins to depend on the density distribution of electrons along the beams. The presented τ values correspond to the increase of A_o for 20 $\div$ 30%. The values of A_o in table 5 are calculated in the Gaussian model of linear density (22). In model (21) with uniform linear density the corresponding values of A_0 are slightly smaller *).

Table 5

	E GeV	laser	b, cm	Δ(B=2T), μm	ω_m, GeV	a_γ, μm	τ, ps	A_0, J
SLC, ν=180 Hz	50	Nd	5	15	24	20	30	15
			< 0.6	< 0.2		< 3	< 7	0.8
		3Nd	5	15	36	20	100	85
VLEPP, ν = 10 Hz	100	Nd	10	30	64	20	25	14
	150	Nd	10	20	109	20	25	17
			< 3	< 2		< 4	< 12	2.3
	300	Nd	10	10	253	20	25	24

The necessary repetition rate ν =10 or 180 Hz is realized up to now at somewhat smaller energies than in table 5 - see table 6.

Table 6

A, J	2.7	5	0.2
ν, Hz	10	7	1000
λ, μm	1.06	0.7÷0.8	0.249
reference	[18]	[19]	[20]

9.3. Possibilities of relaxation of requirements to lasers

It is useful to note that there exists notable reserve to reduce demands upon lasers in comparison with the results of table 5.

*) The presented value of A_0 for E = 150 GeV and b = 10 cm is approximately half as large as the cautious estimation of ref. [1].

Flash energy A and repetition rate ν. The rate of hadron production in the $\gamma\gamma$-collisions is proportional to the product $\nu k^2 \sigma_{\gamma\gamma\to h}$. The cross section of the reaction $\gamma\gamma\to$ hadrons $\sigma_{\gamma\gamma\to h} \approx (2\div 4)\cdot 10^{-31}\,cm^2$, that is $4\div 5$ orders of magnitude larger than that for e^+e^--annihilation in the same region of energy. Therefore, the $\gamma\gamma$-collisions are of great interest already at $L_{\gamma\gamma} \approx 10^{-2} L_{ee}$, i.e.

$$A = (1\div 2)\,J, \quad \nu = 180\ Hz \quad (SLC), \quad \nu = 10\ Hz\ (VLEPP) \qquad (48a)$$

or

$$A \approx 10\,J, \quad \nu = 7\,Hz \quad (SLC), \quad \nu = 0.4\ Hz\ (VLEPP). \qquad (48b)$$

Time duration of laser flash τ. In fig. 12 the dependence of A_0 on τ is shown, calculated in model (22). (Model (21) gives similar curve). It is seen that as τ decreases, the value of A_0 decreases but slightly. With τ increase the value of A_0 grows slowly at first, and then $A_0 \propto \tau$ (19) (here A_0 becomes b-independent). Correspondingly, the required power of a laser P_0 decreases with τ increase and then becomes constant (19d). In particular, at $\tau = 1\,ns$ and $A = 60\,J$ there is quite acceptable conversion coefficient $k = 0.3$. This fact is of interest because some lasers which are perspective for obtaining high repetition rate (with $\omega_0 \gtrsim 1\,eV$) operate in the range of $\tau \gtrsim 1\,ns$ (see sect. 10).

Focal spot radius a_γ. In fig. 13 the dependence of A_0 on the focal spot radius a_γ calculated in model (22) is shown. It is seen that A_0 has a minimum at a certain value of $a_\gamma < r_e$. With a_γ decrease, the energy A_0 grows due to the decrease of the conversion length. At a_γ growth, the energy A_0 grows as a_γ^2 (see (17b)).

Beams. If the diffraction focusing has not been achieved, i.e. the value β_γ (13) is smaller than that given by eq. (14), then in eqs. (16)÷(19) one should use just the real value of β_γ. As a result, the range of validity of the short bunch approximation narrows and it becomes invalid for the obtaining of results at b = 5÷10 cm. The correct formulae for long bucnh approximation in this case are (18b), (19b), i.e. (18c), (19c) should be multiplied by $2\pi a_\gamma^2/\lambda\beta_\gamma$.

If the beams are not Gaussian, then all the results pre-

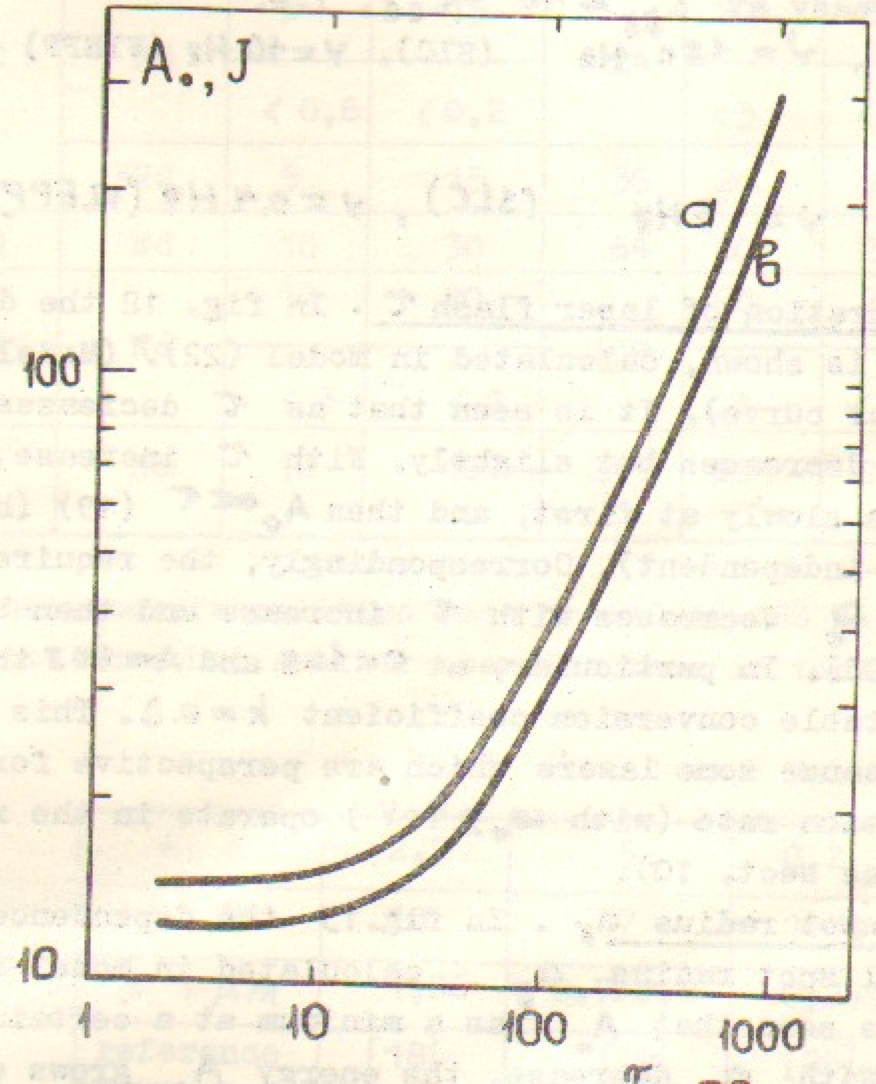

Fig.12. Dependence of the laser flash energy A_o (22) on the flash duration τ at $\omega_o = 1.17$ eV. Curves:

a) VLEPP, E= 150 GeV, $r_e = 13\mu m$, $a_\gamma = 20\mu m$;

b) SLC, E=50 GeV, $r_e = a_\gamma = 20\mu m$.

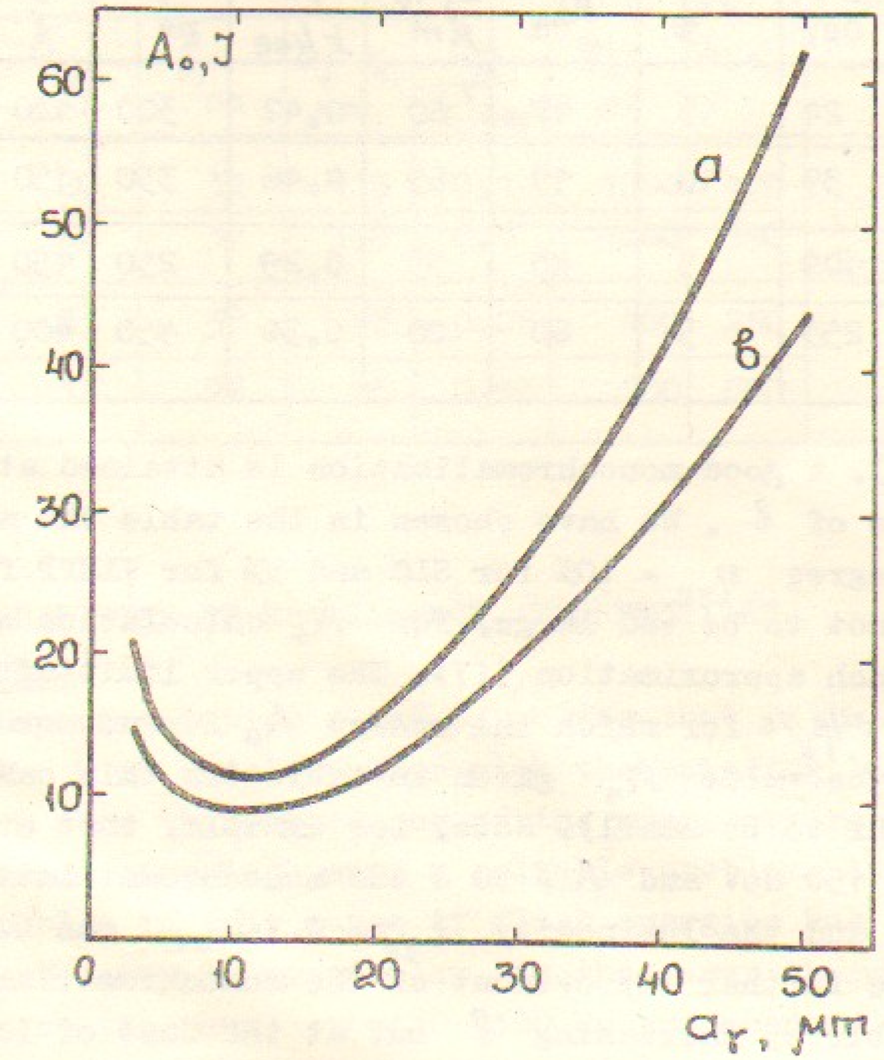

Fig.13 Dependence of the laser flash energy A_o(22) on the laser focal spot radius a_γ at $c\tau = \ell_e$, $\omega_o = 1.17$ eV. Curves:

a) VLEPP, E=150 GeV, r_e =13μm;

b) SLC, E=50 GeV, r_e =20μm.

sented here become estimations only.

9.4. Monochromatization of the γe -collisions

The main data for this case can be found in figs. 6,7,11. Some of the characteristic figures are presented in table 7 for

Table 7

E, GeV	ω_m, GeV	$\eta_{\gamma e}$, %	b, cm	$a_\gamma = r_e$, μm	$L_{\gamma e}/kL_{ee}$	τ, ps	A_0, J	
50	24	10	17	60	0.42	300	120	SLC
70	39	10	19	65	0.46	350	150	ν =180Hz
150	109	5	45	55	0.29	250	150	VLEPP
300	253	5	60	80	0.36	450	400	ν =10Hz

laser (3). A good monochromatization is attained at not too large values of b. We have chosen in the table the monochromatization degree $\eta_{\gamma e}$ = 10% for SLC and 5% for VLEPP for the energy A_0 not to be too large. For A_0 calculation we used the short bunch approximation (17). The upper limit of τ was chosen as $\tau < 4\beta_\gamma/c$ for which the energy A_0 for no more than $20 \div 30\%$ exceeds the value A_0 given in table (in this case parameters (32) occur to be small). Note, for example, that at VLEPP energy E = 150 GeV and A = 50 J the monochromatization degree $\eta_{\gamma e}$ = 5% and the luminosity $L_{\gamma e} = 0.1 \cdot L_{ee}$ can be obtained.

Here further improvement of the monochromatization degree is possible by increasing b but at the cost of luminosity decrease (fig. 7) and A_0 growth (fig. 11).

9.5. Monochromatization of the $\gamma\gamma$ -collisions

The main data for this case can be found in figs. 8,9,11. Some of the characteristic figures for laser (3) are presented in table 8. We have chosen in the table the value $\eta_{\gamma\gamma}$ = 20% for SLC and 15% for VLEPP, having in mind that as b grows, the monochromatization improves very slowly, but the luminosity rapidly drops. As above, for the calculation of A_0 we used the short bunch approximation (17). The upper limit of τ was chosen from the conditions that the parameter (32) is small and $\tau < 4\beta_\gamma/c$.

Note that for obtaining the monochromatic γe- and $\gamma\gamma$-collisions the lasers are needed with the flash energy exceeding that without monochromatization by factor $10 \div 50$. However, here one can use the lasers with considerable larger pulse duration $\tau \sim 1ns$, i.e. to use new types of lasers in comparison with (3).

Table 8

E, GeV	ω_m, GeV	$\eta_{\gamma\gamma}$, %	b, cm	$a_\gamma = r_e$, μm	$L_{\gamma\gamma}/k^2 L_{ee}$	τ, ps	A_0, J	
50	24	20	32	115	0.1	1000	400	SLC
70	39	20	37	130	0.1	1000	590	
150	109	15	58	73	0.08	400	250	VLEPP
300	253	15	77	96	0.13	700	600	

10. POSSIBILITIES OF REALIZATION. PERSPECTIVES

10.1. Lasers

So, by comparing tables 4 and 5, we see that it is possible to obtain $k \sim 1$ in single pulses with the existing lasers. Data of table 6 show that obtaining of the necessary repetition rate at such flash energies seems a solvable problem. Apparently, similar problem in this range of flash energies has not been raised up to now. In particular, in the laser thermonuclear program, where the same $\nu \sim 10 \div 100$ Hz are needed, the main problem now is to obtain the largest energies in one pulse.

For the monochromatization of the γe - and $\gamma\gamma$ -collisions considerably larger values of the energy are needed - see tables 7 and 8. However, such energies do not seem unreachable. In table 9 we present parameters of lasers [21], developed in the framework of the program on the laser thermonuclear synthesis (for multibeam system the energy of one beam is given). All the lasers, except Asterix 3, are made on the basis of neodymium glass or garnet, the latter operates on an iodine vapours.

It is useful to note that one can use $10 \div 20$ synchronized lasers with correspondingly smaller energies at the same repe-

Table 9

Name of the laser (country)	A, J	τ, ps
Argus (USA)	1000	$30 \div 1000$
Gekko (Japan)	1000	$100 \div 1000$
(England, Oldermaston)	500	$50 \div 1000$
Asterix 3 (FRG)	$300 \rightarrow 2000$	300
Mishen 2 (USSR)	250	

tition rate or with the same energies but lower repetition rate.

Of course, for realization of the proposed scheme special lasers should be designed. In particular, one can speak about lasers on neodymium (in glasses or garnet) discussed above.

The first promising results are obtained on lasers using Cr in alexandrite [19] (see table 6). These lasers are perspective for obtaining high repetition rate due to high heat conductivity of alexandrite that makes cooling easier.

Gas lasers (eximer lasers on $XeCl$, KrF and lasers on iodine vapours - see Asterix 3 in table 9) are of interest. Here, the large flash energy can be obtained and the cooling problems restricting repetition rate are much easier than those in the solid state lasers. However, the pulse duration of such lasers is $\gtrsim 1ns$ so far.

The lasers on CO_2 have all the necessary parameters A, τ, a_γ, ν. However, their wave length $\lambda = 10 \mu m (\omega_0 \approx 0.1 eV)$ is too large and $\omega_m \leq 0.35E$ at the energy region considered.

Finally, one should point out the very interesting paper [22] where the laser on free electrons of the same beam is proposed to realize the scheme we have proposed [1, 2]. Using such a laser one has a number of advantages: here only the accelerator technique is used, beam lengths are in accordance and the problem of synchronization is simple.

10.2. Electron beams

Up to now only the laser possibilities were discussed. It is clear, however, that electron beams for the γe - and $\gamma\gamma$ - collisions should be prepared differently than for the e^+e^- - collisions. In particular, it is preferable in the proposed scheme to have electron beams with round cross section but not with elliptic ones as is assumed in the VLEPP project.

Besides, instead of the positron beam one can use an electron beam.

In the e^+e^- -collisions the beam sizes in the interaction region cannot be made very small due to the charged beam interaction. The γe - and $\gamma\gamma$ -collisions are free of such effects and, therefore, their luminosity can be larger than the luminosity of the e^+e^--collisions.

Consider a few examples of luminosity dependence on the beam parameters. Instead of a_e and β_e, we use β_e and emittance

$$\varepsilon = a_e^2 / 2\beta_e , \qquad (49)$$

assuming that β_e is a more flexible parameter than ε.

The necessity of the magnetic deflection of electrons after conversion restricts from below the distance b at the level $5 \div 10$ cm. It is seen from table 5 that at such b the energy A_0 is not too large. Therefore, it is natural to assume the conversion coefficient $k = A/A_0$ to be fixed. Under this condition the luminosity $L_{\gamma e}$, $L_{\gamma\gamma} \propto (\varepsilon\beta_e)^{-1}$, i.e. they can be increased by decreasing β_e. However, at $\beta_e \leq l_e/2$ the luminosity growth slows down.

More intersting possibilities arise in the monochromatic situation when the parameter b can be changed. As we have seen in subsect. 9.4, the values of A_0 are large enough, therefore, it is natural to consider the energy A to be fixed. Moreover, we assume the monochromatization degree η to be fixed which is defined by the parameter (see sect. 7)

$$\rho^2 = \left(\frac{b\theta_0}{a_e} \right)^2 = \frac{b^2\theta_0^2}{2\beta_e\varepsilon} . \qquad (50)$$

To determine A_0 one can use here the short bunch approximation (17). At $a_\gamma \propto r_e$ the energy $A_0 \propto \varepsilon b^2/\beta_e$. In this case, in accordance with (50), the energy $A_0 \propto \varepsilon^2$ and the conversion coefficient $k = A/A_0 \propto \varepsilon^{-2}$ as well do not depend on b and β_e, and the luminosities are

$$L_{\gamma e} \propto A N_e^2 / \varepsilon^3 \beta_e , \quad L_{\gamma\gamma} \propto A^2 N_e^2 / \varepsilon^5 \beta_e . \qquad (51)$$

Hence, as before, the luminosities $L_{\gamma e}$ and $L_{\gamma\gamma}$ can be increased by decreasing β_e, however, in this case the increasing of A is not needed. As before, the growth of the luminosity slows at $\beta_e \lesssim l_e/2$.

Let us emphasize that luminosities (51) strongly depend on the emittance ε. Even a little decreasing of ε leads to considerable $L_{\gamma e}$ and $L_{\gamma\gamma}$ growth. Therefore, one can try to get the gain in the luminosity by decreasing ε even at the cost of decrease of the number of electrons N_e in the beam.

We would like to thank V.E.Balakin, K.G.Folin, A.S.Gainer, A.M.Kondratenko, A.M.Rubenchik, E.L.Saldin, V.A.Sidorov, A.N. Skrinsky, V.D.Ugozhaev, T.A.Vsevolozhskaya, M.S.Zolotorev for very useful discussions. We are very thankful to A.S.Gainer and V.D.Ugozhaev for the composition of bibliography devoted to powerful lasers.

APPENDIX A. COMPARISON OF THE PROPOSED SCHEME WITH THE EQUIVALENT PHOTON SCHEME *)

In the usual e^+e^--collisions one can investigate the $\gamma^* e$- and $\gamma^*\gamma^*$-collisions as well (γ^* is the virtual photon) by means of the scheme of figs. 14 and 15 (see review [23]).

Here, in principle, the virtual photon energy ω is limited by the electron energy E only, and, therefore, ω may be larger than the real photon energy in the proposed scheme. Besides, by means of virtual photons one can investigate the cross section dependence on the "photon masses" q_i^2. However, the corresponding $\gamma^* e$ - and $\gamma^*\gamma^*$-luminosities are small both at large ω and especially at large $|q_i^2|$.

The main part of equivalent photons consists of almost real photons with small $|q_i^2|$. However, in the main region $\omega_m/2 < \omega < \omega_m$ at $k \sim 1$ the luminosity of the proposed scheme is by some orders of magnitude larger than that of the equivalent photons both for the γe - and $\gamma\gamma$ -collisions.

The spectral luminosity for the process of fig. 14 is

$$dL_{\gamma^* e} = L_{ee}\, dn(y) = L_{ee} \frac{\alpha}{\pi} \frac{dy}{y} \left(1 - y + \frac{1}{2} y^2\right) \ln \frac{q_m^2}{m_e^2 y^2} \qquad (A.1)$$

where $y = \omega/E$ and $q_m^2 \approx m_\rho^2$ for the processes of hadron production. In contrast with $dL_{\gamma e}$ (29) the luminosity $dL_{\gamma^* e}$ decreases with y growth (cf. fig. 3). The ratio of these luminosities at $y = y_m$ is

$$\left.\frac{dL_{\gamma^* e}/dy}{dL_{\gamma e}/dy}\right|_{y=y_m} = \frac{\alpha}{4\pi} \frac{\sigma_c}{k\sigma_o} \ln \frac{q_m^2}{m_e^2} \approx \frac{1}{100k}. \qquad (A.2)$$

Spectral luminosity of the equivalent photons $(dL_{\gamma^* e}/dy)/L_{ee}$ as well as that of the proposed scheme $(dL_{\gamma e}/dy)/kL_{ee} = f(x,y)$ (6a) are presented in fig. 16 for E = 150 GeV and ω_o = 1.17 eV. It is seen that they are equal at very small y = 0.033 or ω = = 5 GeV (note that ω_m = 109 GeV). The ratio of the $\gamma^* e$ -luminosity integrated over $y > y_m/2$ to that in the γe -collisions is $(0.065 \div 0.025)/k$ for $E = 50 \div 300$ GeV.

The ratio of the $\gamma^*\gamma^*$- and $\gamma\gamma$ -luminosities is still much smaller. The $\gamma^*\gamma^*$-luminosity (cf. (A.1)) is $dL_{\gamma^*\gamma^*} = L_{ee} \cdot dn(y_1)\, dn(y_2)$, and hence we have (see [23])

---

*) In Appendices we use the units where $\hbar = c = 1$.

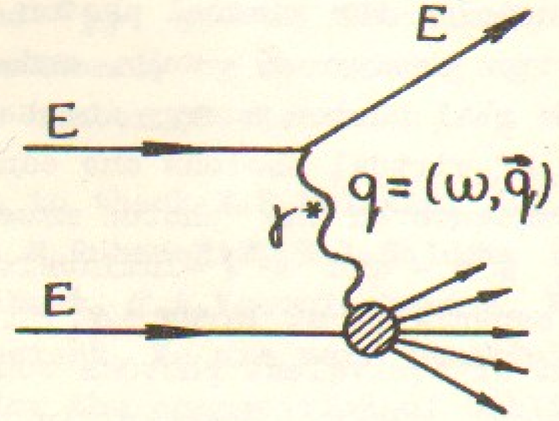

Fig.14. The $\gamma^* e$ - collisions in the $e^{\pm}e^-$ - beams.

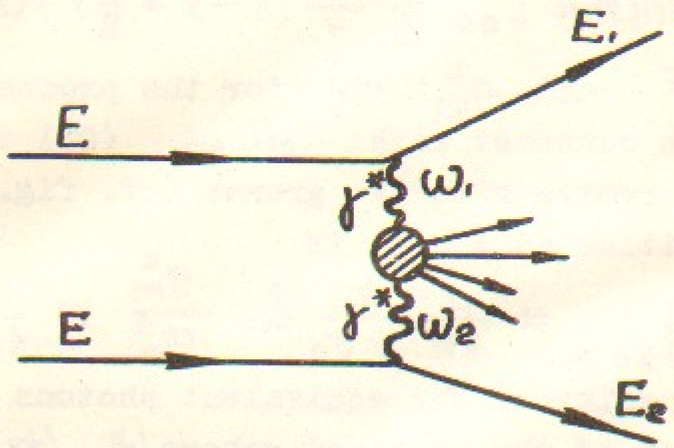

Fig.15. The $\gamma^*\gamma^*$ - collisions in the $e^{\pm}e^-$ -beams.

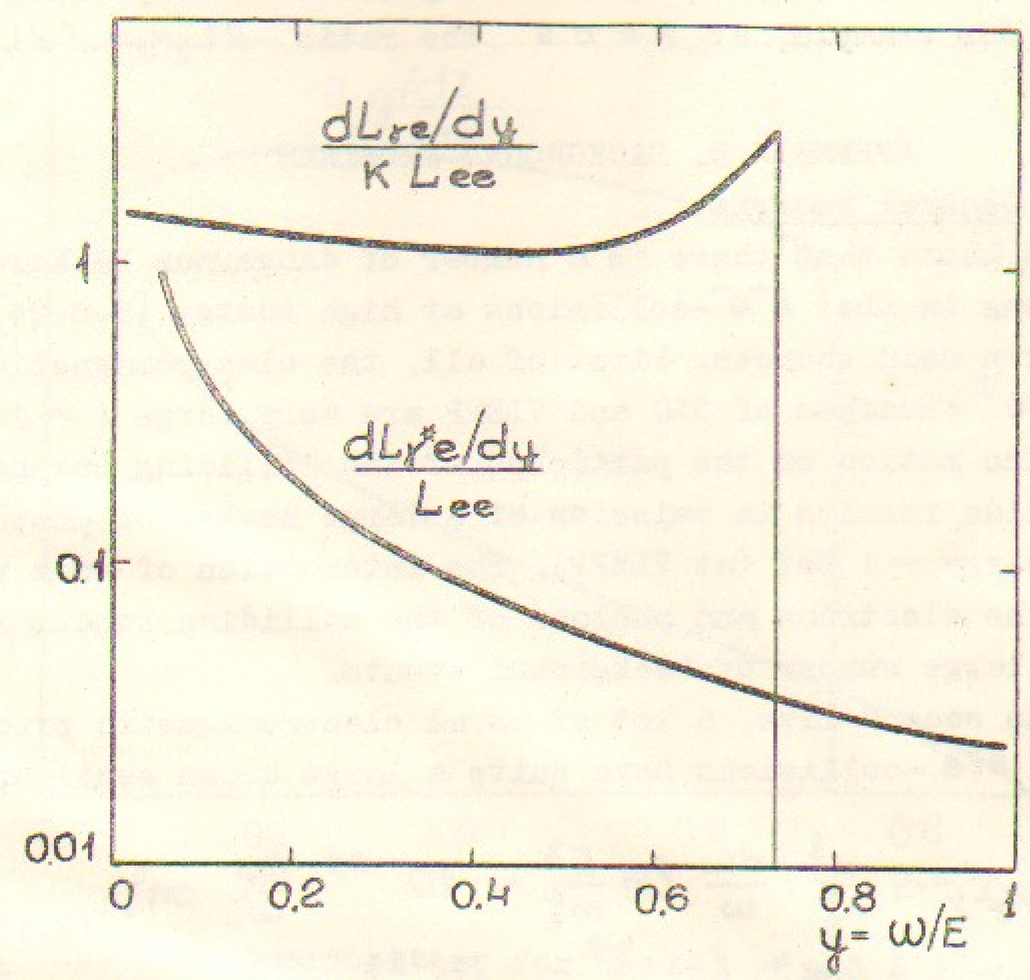

Fig.16. Spectral luminosities for the γe - and $\gamma^* e$ -collisions at E= 150 GeV, ω_0 = 1.17 eV.

$$\frac{1}{L_{ee}}\frac{dL_{\gamma^*\gamma^*}}{dz} = \frac{\alpha^2}{\pi^2}\frac{2}{z}\left\{\left[2\left(1+\frac{1}{2}z^2\right)\ln\frac{1}{z} - \frac{1}{2}(1-z^2)(3+z^2)\right]\left(\ln\frac{q_m^2}{m_e^2 z^2}\right)^2 - \frac{8}{3}\ln^3\frac{1}{z}\right\}, \quad z = \frac{W_{\gamma\gamma}}{2E}. \tag{A.3}$$

The graphs of this function and the function $(dL_{\gamma\gamma}/dz)/k^2L_{ee}$ (30) are presented in fig. 17 for the abovementioned example. It is seen that the luminosity of equivalent photons is very small at large z. For example, at $z = 0.6$ the ratio $dL_{\gamma^*\gamma^*}/dL_{\gamma\gamma} \sim 10^{-3}/k^2$.

APPENDIX B. BACKGROUND PROBLEMS

B.1. General remarks.

It is known that there is a number of dangerous background processes in the e^+e^--collisions at high energy [5,8,24]. They have two main sources. First of all, the electromagnetic fields of $e^{\pm}$-bunches of SLC and VLEPP are very large ($\sim 10 \div 100$ T). The motion of the particles of the colliding bunches in such fields results in emission of a large number of photons with the energy ~ 1 GeV (at VLEPP). The interaction of such photons with the electrons and photons of the colliding bunch results in a large number of background events.

In the second line, a lot of usual electromagnetic processes in the e^+e^--collisions have quite a large cross section, e.g.,

$$d\sigma_{e^+e^-\to e^+e^-\gamma} \sim \frac{\alpha^3}{m_e^2}\frac{d\omega}{\omega}\ln\frac{E^2}{m_e^2} \sim 10^{-26}\frac{d\omega}{\omega}\ cm^2, \tag{B.1}$$

$$\sigma_{e^+e^-\to e^+e^-e^+e^-} \sim \frac{\alpha^4}{m_e^2}\ln^3\frac{E^2}{m_e^2} \sim 10^{-26}\ cm^2.$$

These cross sections are many orders of magnitude larger than those for processes of interest.

For the proposed $\gamma\gamma$ - and γe-collisions the background situation seems much more favourable. The first source of background is absent, besides, the main background processes in the $\gamma\gamma$ -collisions have small cross sections. However, there are additional background processes which are connected with the proposed conversion scheme. It seems that one can make them not dangerous. Let us discuss the latter question.

B.2. Removal of electrons after conversion

After conversion the electrons are bent by the magnetic field. If they strike the walls of the vacuum chamber, that

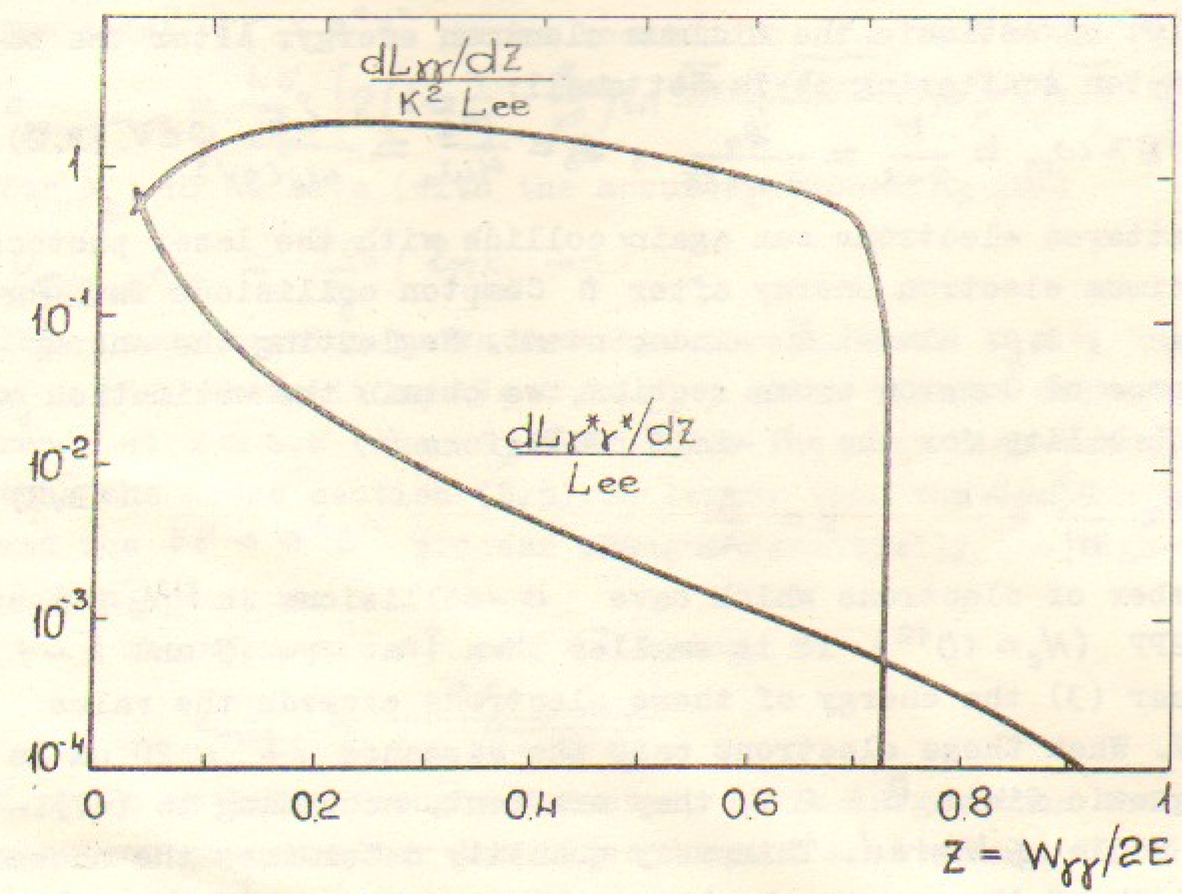

Fig.17. Spectral luminosities for the $\gamma\gamma$ - and $\gamma^*\gamma^*$-collisions at $E = 150$ GeV, $\omega_0 = 1.17$ eV.

would lead to a large number of background events. To avoid that, one should remove them from the system, using the fact that all of them fly in one plane (independently of their energies). So, it is sufficient to enlarge the vacuum chamber in this plane. The width of this part of vacuum chamber must be wide enough to avoid the collision of the slowest electrons with the chamber walls.

Let us estimate the minimum electron energy. After the basic Compton scattering it is not small:

$$\mathcal{E}_{min} = E - \omega_m = \frac{E}{x+1} = \frac{\mathcal{E}_o}{1+1/x}, \quad \mathcal{E}_o = \frac{m_e^2}{4\omega_o} = \frac{65}{\omega_o(eV)}\ GeV. \tag{B.2}$$

The scattered electrons can again collide with the laser photons. The minimum electron energy after n Compton collisions is $E/(nx+1) \approx \mathcal{E}_o/n$, i.e. almost E -independent. Neglecting the energy dependence of Compton cross section, we obtain the estimation of the probability for the n-fold collisions

$$P \approx \frac{k^n}{n!} e^{-k}, \quad k = \frac{A}{A_o}. \tag{B.3}$$

The number of electrons which have n-collisions is PN_e, i.e. for VLEPP ($N_e = 10^{12}$) it is smaller than 1 at $n = 15$ and $k \sim 1$. For laser (3) the energy of these electrons exceeds the value 3.5 GeV. When these electrons pass the distance $2b$ = 20 cm in the magnetic field B = 2 T, they are bent, according to (47), at the angle $\lesssim 4 mrad$. This very quantity determines the necessary width of the vacuum chamber.

B.3. Compton scattered photons striking chamber walls

The photons which scatter in the conversion region at large angles, can give the background events striking the vacuum chamber walls. However, in this case their energies are small, and all of them can be absorbed by a thin layer of absorber. Indeed, according to (4), the energy of the photon which flies at an angle $\theta \gg \theta_o$ is small: $\omega = 4\omega_o/\theta^2$, and the number of the photons with $\theta > \theta_{min}$ is $kN_e(\sigma_o/\sigma_c)(2m_e/E\theta_{min})^2$. If we choose small enough value of $\theta_{min} = 5\ mrad$, we obtain $\omega <$ <200 keV for laser (3), and the number of these photons at E = 150 GeV does not exceed $10^{-6} kN_e$.

B.4. The $\gamma\gamma \to e^+e^-$ process in the conversion region

When the value $x = 4E\omega_o/m_e^2$ grows, some other processes in the conversion region become important (besides the basic Compton scattering) - cf. sect. 8. The main of them is the e^+e^--production at the collision of a high-energy photon with the laser one. Invariant mass of this system is $W = \sqrt{4\omega\omega_o}$. Since $\omega < Ex/(x+1)$, the threshold value of $W = 2m_e$ can only be achieved at

$$x > 2(1+\sqrt{2}) \approx 4.8 \tag{B.4}$$

The total $\gamma\gamma \to e^+e^-$ cross section is $(x_\gamma = 4\omega\omega_o/m_e^2)$

$$\sigma_{\gamma\gamma\to e^+e^-} = \frac{4\sigma_o}{x_\gamma}\left[2\left(1+\frac{4}{x_\gamma}-\frac{8}{x_\gamma^2}\right)\ln\frac{\sqrt{x_\gamma}+\sqrt{x_\gamma-4}}{2} - \left(1+\frac{4}{x_\gamma}\right)\sqrt{1-\frac{4}{x_\gamma}}\right]. \tag{B.5}$$

For $x_\gamma > 10$ we have (with the accuracy exceeding 20%)

$$\sigma_{\gamma\gamma\to e^+e^-} \approx \frac{4\sigma_o}{x_\gamma}(\ln x_\gamma - 1) \tag{B.6}$$

This cross section grows from the threshold at $x_\gamma = 4$ up to $x_\gamma \approx 8$, where it equals $\approx 0.7\sigma_o$, after that it decreases. Already at $x \approx 6.8$ (when $x_\gamma \lesssim 6$) for the most high-energy photons the cross section (B.5) is larger than the Compton one (5), and the $\gamma\gamma \to e^+e^-$ process changes essentially the high-energy photon spectrum.

The minimum e^+ or e^- energy is

$$\mathcal{E}_{min} = \frac{2\mathcal{E}_o}{1+\sqrt{1-4/x_\gamma}} \tag{B.7}$$

i.e. it is large enough. Moreover, it is larger than the minimum electron energy after the first Compton scattering. The escape angles of $e^\pm$ are very small

$$\theta_\pm < \frac{2\omega_o}{m_e} \sim 10^{-5}. \tag{B.8}$$

After the magnetic deflection these electrons are removed together with the Compton ones. For the removal of positrons it is necessary to enlarge the vacuum chamber in the direction symmetric to electrons.

The electromagnetic fields in the conversion region are very strong, this can lead to notable nonlinear effects [25].

In particular, the e^+e^--production is possible even at x < 4.8. However, the number of such e^+e^--pairs at the quantities considered is some orders of magnitude smaller than at 4.8, and the $e^\pm$ energy is large enough.

B.5. The collisions of deflected electron bunch with the electrons and photons of the colliding bunch

The electrons which conserved their energy E have the minimal deflections. They have Gaussian distribution with the r.m.s radius $\sim a_e$. (The electrons with lower energy have larger deflections and they are unessential). Due to the deflection at the distance Δ (47) the collision number of these electrons with the electrons of the colliding bunch decreases by a factor $\exp(-\Delta^2/2a_e^2)$ for the γe -collisions and by a factor $\exp(-2\Delta^2/a_e^2)$ for the $\gamma\gamma$ -collisions. For the figures of table 5 the minimal value of $\Delta/a_e \approx 8$, which corresponds to $\exp(-\Delta^2/2a_e^2) \sim 10^{-14}$.

In the scheme of the $\gamma\gamma$ -collisions much more dangerous are the collisions between the deflected electrons with the photons of the colliding bunch, which fly at the angle $\theta \approx \Delta/b$ inside the solid angle $\Delta\Omega \approx \pi a_e^2/b^2$. But the energy of these photons is not large, $\omega = \omega_m \cdot (\theta_0/\theta)^2 = 4\omega_0/\theta^2$, and the effective luminosity of these collisions is small, $\sim k(1-k)L_{ee}(b\theta_0/\Delta)^2(a_e/\Delta)^2$. In these collisions the process $e\gamma \to e e^+e^-$ has the largest cross section, $\sim 4\cdot 10^{-26}$ cm (see below). From here one can obtain that the number of such events per one collision $\lesssim 10^{-2}$ for SLC and $\lesssim 2$ for VLEPP, besides, $\omega < 0.5$ GeV and the energy of every e^+ or e^- is less than ω.

B.6. The collisions of positrons from the collision region with the electrons of the colliding bunch (for the $\gamma\gamma$ -collisions)

At $x > 4.8$ the process $\gamma\gamma \to e^+e^-$ in the conversion region produces a lot of positrons (see subsection B.3). They are bent by the magnetic field and can meet, in principle, with the deflected electrons of the colliding bunch. It can give the background processes of the (B.1) type with very large cross sections. However, the maximum energy of these positrons $\varepsilon_{max} = \omega_m - \varepsilon_{min}$ (B.7) is considerable less than E. Therefore, they do not collide with the most dense part of the electron bunch whose electron energy is E. For example, the energy $\varepsilon_{max} < 160$ GeV in the last case of table 5, hence, the most high-energy positrons fly at the distance $\approx 15a_e$ (at B = 2 T) from the most high-energy electrons. As a result, in the collision the beam regions with low densities will take part, and one can hope that the processes (B.1) do not give a considerable background.

Nevertheless, if the number of such events is large, one can exclude them, if we make the magnetic fields from both sides

of the interaction region at some angle to each other.

B.7. Physical background in the γe -collision. The Bethe-Heitler processes $\gamma e \to e^+e^-e$, $\gamma e \to \mu^+\mu^-e$

In the γe -collisions the process of the lowest order in α - the Compton effect - has the small cross section (5) at the energies under consideration $\sigma_c \lesssim 10^{-33}$ cm^2, and it is unimportant.

The main background process is Bethe-Heitler production of the e^+e^- -pairs with the large cross section *)

$$\sigma_{\gamma e\to e^+e^-e} = \frac{28}{9\pi}\alpha\sigma_0\left(\ln\frac{4E\omega}{m_e^2} - \frac{109}{42}\right) \sim 4\cdot 10^{-26}\,\mathrm{cm}^2. \quad (B.9)$$

The main contribution in this cross section is due to the region where the incident electron almost conserves its momentum and the produced particles fly along the photon momentum. The transverse momenta of the produced particles (e^+ and e^- or μ^+ and μ^-) $k_{1\perp}$ and $k_{2\perp}$ almost compensate each other. The distribution over the transverse momenta of scattered electrons $p_\perp = -k_{1\perp} - k_{2\perp}$ and over the effective mass of the produced pair W has a form (at $p_\perp^2 \ll W^2 \ll 4E\omega_0$)

$$\frac{d\sigma}{dp_\perp^2 dW^2} = \frac{4\alpha^3}{W^4}\left(\ln\frac{W^2}{m_\ell^2} - 1\right)\cdot\frac{p_\perp^2}{[p_\perp^2 + m_e^2W^4/(4E\omega)^2]^2} \quad (B.11)$$

After integration over $p_\perp$ we have

$$\frac{d\sigma}{dW^2} = \frac{4\alpha^3}{W^4}\left(\ln\frac{16E^2\omega^2}{m_e^2W^2} - 1\right)\left(\ln\frac{W^2}{m_\ell^2} - 1\right), \quad 4E\omega \gg W^2 > m_\ell^2 \quad (B.12)$$

From here one can easily obtain the production cross section of the pairs with the effective masses larger than W_0 (at $m_\ell^2 \ll W_0^2 \ll 4E\omega$)

$$\sigma(W>W_0) = \frac{4\alpha^3}{W_0^2}\ln\frac{W_0^2}{m_\ell^2}\ln\frac{16E^2\omega^2}{m_e^2W_0^2}. \quad (B.13)$$

---

*) With logarithmic accuracy one can describe the cross sections of the reactions $\gamma e \to \ell^+\ell^- e$ ($\ell = \mu, \tau$) by the relation of the (B.9) type

$$\sigma_{\gamma e\to \ell^+\ell^- e} = \frac{28}{9}\frac{\alpha^3}{m_\ell^2}\ln\frac{4E\omega}{m_e m_\ell}. \quad (B.10)$$

It gives at $\omega \sim E \sim 50 \div 300$ GeV,

$$\sigma_{\gamma e\to\mu^+\mu^-e} \sim 8\cdot 10^{-31}\,\mathrm{cm}^2; \quad \sigma_{\gamma e\to\tau^+\tau^-e} \sim 2\cdot 10^{-33}\,\mathrm{cm}^2. \quad (B.10a)$$

The effective mass of the $\ell^+\ell^-$-pair is $W=\sqrt{4\omega\Delta E}$ where ΔE is the energy loss of the scattered electron. Therefore, eq. (B.13) is the ΔE-distribution as well. In the same way, if the scattered electron has the transverse momentum larger than $p_\perp$, the corresponding cross section has the form of the (B.13) type with $W_0 \sim p_\perp$. As a result, at $\Delta E \gtrsim$ 1 GeV or $p_\perp \gtrsim 1$ GeV the cross section decreases by a factor of 10^{-6} at least.

If the e^+ (or e^- or $\mu^\pm$) flies at the angle $\theta_{th} < \theta < \pi/2$ to the photon momentum and with the energy $\varepsilon > \varepsilon_{th}$, the corresponding cross section is [24]

$$\sigma(\varepsilon > \varepsilon_{th}, \theta > \theta_{th}) \approx \frac{2\alpha^3}{\omega \varepsilon_{th} \theta_{th}^2} \ln \frac{\varepsilon^2}{m_e^2 \theta_{th}^2} . \qquad (B.14)$$

Therefore, at $\varepsilon_{th}\theta_{th} \gtrsim 1$ GeV the cross section decreases by a factor $\sim 10^{-6}$, i.e. this background can be excluded if we do not detect $e^\pm$ with small energies and flying at small angles.

Other background processes ($\gamma e \to \mu^+\mu^- e$, $\gamma e \to e^+e^-e^+e^-e$, ...) have much smaller cross sections and can be neglected together with the Bethe-Heitler process.

B.8. Physical background in the $\gamma\gamma$-collision. The process $\gamma\gamma \to e^+e^-e^+e^-$.

In the $\gamma\gamma$-collisions the process of the lowest order in α – $\gamma\gamma \to \ell^+\ell^-$, $\ell = e, \mu, \tau$ – has the small cross section $(\pi\alpha^2/\omega_1\omega_2) \ln(\omega_1\omega_2/m_\ell^2) \lesssim 10^{-32}$ cm^2 at the energies under consideration.

The main background process is the production of two e^+e^--pairs [26]:

$$\sigma_{\gamma\gamma \to e^+e^-e^+e^-} = 1.52 \frac{\alpha^4}{m_e^2} = 6.45 \cdot 10^{-30}\ cm^2. \qquad (B.15)$$

The main contribution in this cross section is due to the region where every e^+e^--pair flies along the momentum of "their" photon having small invariant mass $\sim 2m_e$ and total transverse momentum $\sim m_e$. Any removal from this region decreases very sharply this cross section and makes it unimportant (in the way similar to that for the Bethe-Heitler process, sect. B.7).

APPENDIX C. LUMINOSITY CALIBRATION

The proposed scheme demands the calibration of the luminosity. This problem here is more difficult than in e^+e^-, ep or pp colliding beams because in our case one needs the calibration both of the total and the spectral luminosity.

C.1. γe-collisions

For the calibration of the γe-collisions one can use the e^+e^-- or $\mu^+\mu^-$-pair production ($\gamma e \to e^+e^-e$, $\mu^+\mu^-e$). We described them in subsect. B.7. Let us remind that the total cross sections of these processes (B.9), (B.10) at the energies under consideration are weakly energy dependent and are $\sim 4\cdot 10^{-26} cm^2$ for $\gamma e \to e^+e^-e$ and $\sim 8\cdot 10^{-31} cm^2$ for $\gamma e \to \mu^+\mu^-e$ process. The produced particles fly along the photon momentum and their total energy equals ω. Therefore, the total luminosity is proportional to the total number of produced electrons or muons, and the distribution over photon energy (the spectral luminosity) coincides with that over the total energy of the e^+e^-- or $\mu^+\mu^-$-pair.

The spectrum of the produced particles is (cf. [13])

$$d\sigma = \frac{4\alpha^3}{m_\ell^2} \frac{d\varepsilon_+}{\omega^3} \left(\varepsilon_+^2 + \varepsilon_-^2 + \frac{2}{3}\varepsilon_+\varepsilon_-\right)\left(\ln \frac{2\varepsilon_+\varepsilon_- E}{m_e^2 \omega} - \frac{1}{2}\right). \qquad (C.1)$$

Here $\ell = e$ or μ, $\varepsilon_\pm$ is the $\ell^\pm$-energy, $\omega = \varepsilon_+ + \varepsilon_-$.

To obtain the spectral luminosity, it is sufficient to measure the energy spectrum of $\mu^\pm$ or $e^\pm$, but muons are more convenient due to small background.

One can also detect the electrons or muons which are scattered at the angle 10–100 mrad. If the $\mu^\pm$ or $e^\pm$ fly at the angle $\theta > \theta_{th}$ and with the energy $\varepsilon > \varepsilon_{th}$, the corresponding cross section (B.14) is $\approx 10^{-32} cm^2 \cdot [\varepsilon(GeV)\,\omega(GeV)\,\theta_{th}^2]^{-1}$. It gives, e.g., approximately 1 event per second for SLC at $k \sim 1$, $\varepsilon_{th} \sim 1$ GeV, $\theta_{th} \sim$ 30 mrad.

Studying the processes with small cross sections, one can use for calibration the Compton effect. Its cross section is (after integration over scattering angles of electrons $\theta_e > \theta_{th}$)

$$\sigma_{\gamma e \to \gamma e} = \frac{1.3 \cdot 10^{-31} cm^2}{W_{\gamma e}^2\ (GeV^2)} \cdot \ln \frac{1}{\theta_{th}^2}, \quad (10^{-5} \ll \theta_{th} < 0.5). \qquad (C.2)$$

The incident photon energy is determined in this case by the energy and the escape angle of scattered electron.

C.2. $\gamma\gamma$-collisions

For the calibration of the $\gamma\gamma$-collisions one can use the processes $\gamma\gamma \to e^+e^-e^+e^-$ (σ = $6.5 \cdot 10^{-30}$ cm^2) or $\gamma\gamma \to \mu^+\mu^-e^+e^-$ ($\sigma \approx 5.7 \cdot 10^{-33}$ cm^2 [27]). The cross sections of these processes do not depend on the energy. The particles of every pair fly along the momentum of "their" photon and the total pair energy equals the energy of this photon. (For comparison, point out that among the processes of interest the $\gamma\gamma \to$ hadrons transition has the maximum cross section $\sigma_{\gamma\gamma\to h} = (2\div 4)\cdot 10^{-31}\ cm^2$).

As in the previous case, to obtain the spectral luminosity, it is sufficient to measure the energy spectrum of $\mu^\pm$ or $e^\pm$. At $x > 4.8$ the positrons become unconvenient due to the background from the process $\gamma\gamma \to e^+e^-$ in the conversion region (cf. also [25]).

Studying the processes with small cross sections (e.g., the quark jets $\gamma\gamma \to q\bar{q}$), one can use for calibration the production of one e^+e^- or $\mu^+\mu^-$ -pair. Their cross sections are (after integration over scattering angles $\theta > \theta_{th}$)

$$\sigma_{\gamma\gamma\to e^+e^-} = \sigma_{\gamma\gamma\to\mu^+\mu^-} = \frac{2.6\cdot 10^{-31} cm^2}{W_{\gamma\gamma}^2\,(GeV^2)} \ln\frac{4}{\theta_{th}^2}\,. \qquad (C.3)$$

REFERENCES

1. I.F.Ginzburg, G.L.Kotkin, V.G.Serbo, V.I.Telnov, Preprint INP (Novosibirsk) 81-50 (1981).
2. I.F.Ginzburg, G.L.Kotkin, V.G.Serbo, V.I.Telnov, Pisma ZHETF 9 (1981) 514.
3. V.E.Balakin, A.N.Skrinsky, report, presented V.Amaldi at Inter.Symp. on Lepton and Photon Interactions on High Energies, Bonn, (August, 1981).
4. V.E.Balakin, G.I.Budker, A.N. Skrinsky, Proc. ALL-Union. Conf. on Charged Particles Accelerators, Dubna (1978) p.27; V.E.Balakin, I.A.Koop, A.F.Novokhatsky, A.N.Skrinsky, V.P.Smirnov, ibid, p.143.
5. SLAC-Report-229, 1980; P.Panofsky, Report, presented at International Symposium on Lepton and Photon Interactions on High Energies. Bonn (August, 1981).
6. R.Wedermeyer. Report, presented at abovementioned Symposium; Proc. of the 1V Int. Col. on photon-photon interactions. Paris (1981).
7. Proc. of the LEP Summer Study. CERN 79-01 (1979).
8. Proc. Workshop on Programme of Experiments at Colliding Linear e^+e^- -beams (VLEPP), 1-5 December, 1980, Novosibirsk.
9. A.N.Skrinsky, Int. Seminar on Perspectives in High Energy Physics. Morges, Switzerland (1971).
10. F.A.Arutyunian, V.A.Tumanian, Phys. Lett. 4(1963) 176; F.R.Arutyunian, I.I.Goldman, V.A.Tumanian, ZHETF(USSR) 45 (1963) 312; R.H.Milburn, Phys. Rev. Lett. 10 (1963)75.
11. O.F.Kulikov et al., Phys. Lett. 13 (1964) 344; L.Federici et al., Nuovo chim. 59 (1980) 247.
12. J.Ballam et al., Phys. Rev. Lett. 23 (1969) 498.
13. V.B.Berestecky, E.M.Lifshitz, L.P.Pitaevsky, Quantum electrodynamics (Nauka, Moscow, 1980).
14. G.S.Landsberg, Optics, Moskow (1976).
15. A.N.Skrinsky, Usp. Fiz. Nauk (1982).

16. Laser Focus, June, 1980, p.34.

17. a) K.Tanaka, L.M.Goldman, Phys. Rev. Lett. 45 (1980)1558;
b) V.F.Efimov, I.G.Zubarev et al., Kvant. electronika 6 (1979) 2031;
c) P.D.Cartes, S.M.L.Sim, E.R.Wooding, Optics Comm. 33 (1980) 443.

18. R.M.Kogan, T.G.Crow, Appl. Opt. 17 (1978) 927.

19. J.C.Walling et al., IEEE Jorn. Quant. Electron. QE-16 (1980) 1302.

20. T.S.Fahlen, ibid QE-11 p.1260.

21. C.Yamanaka. Nuclear Fusion 20 (1980) 507.

22. A.M.Kondratenko, E.V.Pakhtusova, E.L.Saldin, preprint INP (Novosibirsk) 81-130 (1981).

23. V.M.Budnev, I.F.Ginzburg, G.V.Meledin, V.G.Serbo, Phys, Reports 15 C (1975) 181.

24. M.S.Zolotorev, E.A.Kuraev, V.G.Serbo, preprint INP (Novosibirsk) 81-63 (1981).

25. G.L.Kotkin, S.I.Politiko, preprint Ins. of Math. (Novosibirsk, 1982).

26. L.N.Lipatov, G.V.Frolov, Sov.J.Nucl. Phys. 13 (1971) 333; H.Cheng, T.T.Wu, Phys. Rev. D1 (1970) 3414.

27. V.G.Serbo, Pis'ma ZhETF 12 (1970) 50, 452.

Работа поступила - 6 августа 1981 г.

Ответственный за выпуск - С.Г.Попов
Подписано к печати 29.12-1981г. МН 03542
Усл. 4,0 печ.л., 3,0 учетно-изд.л.
Тираж 290 экз. Бесплатно
Заказ № 102.

Отпечатано на ротапринте ИЯФ СО АН СССР